HHS Public Access

Author manuscript

J Cell Physiol. Author manuscript; available in PMC 2022 August 01.

Published in final edited form as:

J Cell Physiol. 2021 August ; 236(8): 5937–5952. doi:10.1002/jcp.30279.

Oscillating calcium signals in smooth muscle cells underlie the persistent basal tone of internal anal sphincter

Ping Lu[1], **Jun Chen**[1,Ψ], **Chenghai Zhang**[2], **Dieter Saur**[3], **Christina E Baer**[1,4], **Lawrence M Lifshitz**[5], **Kevin E Fogarty**[5], **Ronghua ZhuGe**[1,Φ]

[1]Department of Microbiology and Physiological Systems, University of Massachusetts Medical School, Worcester, MA, USA

[2]Department of Biological Chemistry and Molecular Pharmacology, Blavatnik Institute at Harvard Medical School, Boston, MA, USA

[3]Department of Internal Medicine II, Klinikum rechts der Isar, Technische Universität München, München, Germany.

[4]Sanderson Center for Optical Experimentation, University of Massachusetts Medical School, Worcester, MA, USA

[5]Program in Molecular Medicine, University of Massachusetts Medical School, Worcester, MA, USA

Abstract

A persistent basal tone in the internal anal sphincter (IAS) is essential for keeping the anal canal closed and fecal continence. Its inhibition via the rectoanal inhibitory reflex (RAIR) is required for successful defecation. However, cellular signals underlying the IAS basal tone remain enigmatic. Here we report the origin and molecular mechanisms of calcium signals that control the IAS basal tone, using a combination approach including a novel IAS slice preparation that retains cell arrangement and architecture as *in vivo,* 2-photon imaging, and cell-specific gene-modified mice. We found that IAS smooth muscle cells generate two forms of contractions (i.e., phasic and sustained contraction) and Ca^{2+} signals (i.e., synchronized Ca^{2+} oscillations (SCaOs) and asynchronized Ca^{2+} oscillations (ACaOs)) that last for hours. RyRs, TMEM16A, L-type Ca^{2+} channels, and gap junctions are required for SCaOs, which account for phasic contraction and 75% of sustained contraction. Nevertheless, only RyRs are required for ACaOs, which contribute 25% of sustained contraction. Nitric oxide, the primary neurotransmitter mediating the RAIR, blocks

[Φ]Corresponding author: Ronghua.zhuge@umassmed.edu.

[Ψ]Present address: Division of Pulmonary Diseases, State Key Laboratory of Biotherapy, and Department of Respiratory and Critical Care Medicine, West China Hospital of Sichuan University, Chengdu, China

CONTRIBUTIONS

P.L., and R.Z. conceived the experiments. P.L., J.C., C.Z., R.Z. designed the study. P.L., J.C. performed the experiments. P.L., J.C., L.L., K.F., and R.Z. analyzed and interpreted the data. D.S. provided reagent. C.B. supervised imaging. L.L and K.F edited the manuscript, and P.L. and R.Z. wrote the manuscript.

ETHICS DECLARATIONS

Competing interests

The authors declare no competing interests.

DATA AVAILABILITY STATEMENT

The data that support the findings of this study are available from the corresponding author upon reasonable request.

both types of Ca^{2+} signals, leading to IAS's full relaxation. Our results show that the oscillating nature of Ca^{2+} signals generates and maintains the basal tone without causing cytotoxicity to IAS. Our study provides insight into fecal continence and normal defecation.

Keywords

Internal anal sphincter; Phasic contraction; Sustained contraction; Calcium oscilations; Ion channels

1 | INTRODUCTION

The anus, located at the end of the gastrointestinal tract, is the gate through which the stool is discharged. Precise opening and closure of the anus are essential for fecal continence, defecation and social well-being (Kumar & Emmanuel, 2017; Madoff & Fleshman, 2004; Rattan & Singh, 2011a; Zbar, Jayne, Mathur, Ambrose, & Guillou, 2000). A malfunction in the anal opening and closure often leads to debilitating disorders such as fecal incontinence and anal fissure (Foxx-Orenstein, Umar, & Crowell). These anal disorders cause significant personal psychological distress and tremendous social and economic burdens. For example, fecal incontinence affects 18 million people and a leading reason for nursing home placement in elderlies in the United States (Bharucha, 2004; Guillaume, Salem, Garcia, & Chander Roland, 2017; Lee, 2014; McCallion & Gardiner, 2001).

In mammals and humans, the anus consists of two muscle sphincters controlled by different cellular and molecular mechanisms(Rao, 2004; Stewart, Cook, Dyer, & Alperin, 2018; Tsukada et al., 2016). The external anal sphincter is a skeletal muscle structure and is innervated by the inferior rectal motor nerve. This sphincter is critical for the voluntary control of defecation while awake. The second sphincter of the anus is smooth muscle and is located in the anal muscle's inner layer, called the internal anal sphincter (IAS). It has been long recognized that the IAS contributes more than 70% of anal pressure at rest, and is critical for maintaining anal canal closure, hence fecal continence during sleep and wakefulness(Rattan, 2005; Rattan & Singh, 2011b). As defecation in humans takes place only one or a few times in 24 hours and each lasts for merely ten seconds, a long-standing, enigmatic and intriguing question has been how the IAS maintains its tone for such prolonged times.

One hypothesis states that IAS smooth muscle cells (IAS-SMCs) express relatively less myosin light chain phosphatase (MLCP), so that myosin light chain is more prone to be phosphorylated by myosin light chain kinase (MLCK), leading to the basal tone(Rattan, 2017). However, the specific ablation of MYPT1, a subunit of MLCP, in the SMCs generates no effect on the basal tone and fecal size, arguing that this mechanism may not play a major role in setting the basal tone of IAS(Zhang et al., 2016). Another hypothesis stresses the role of interstitial cells of Cajal (ICC) in the basal tone generation(C. A.-O. Cobine et al.; C. A. Cobine et al., 2017; Hannigan et al.). It proposes that IAS's ICCs act as the pacemaker with Ca^{2+}-activated Cl^{-} channel TMEM16A serving as a pacemaking channel. The TMEM16A-mediated electrical slow waves in the ICCs propagate into IAS-SMCs, leading to the depolarization and activation of L-type voltage-dependent Ca^{2+} channels (VDCCs) in the

SMCs and the resulting basal tone. However, the ICC hypothesis solely relies on results from the expression of TMEM16A and the use of TMEM16A inhibitors (that block the channel in all cell types in tissues)(C. A. Cobine et al., 2017; Hannigan et al.). It awaits its validation with genetic approaches targeting specific cell types. Finally, we recently demonstrated that the RyR-TMEM16A-VDCC signaling module in IAS-SMCs is required and sets the basal tone. We also found that activation of these three channels raises intracellular Ca^{2+} concentration in single isolated IAS-SMCs(Zhang et al., 2016). As a sustained high level of global calcium would cause cytotoxicity and lead to apoptotic, necrotic, or autophagic cell death(Athamneh et al., 2020; Cerella, Diederich, & Ghibelli, 2010; Zhivotovsky & Orrenius, 2011), Ca^{2+} signals that can maintain the contractile status of IAS-SMCs for hours without causing cell death remained to be discovered. Finding these Ca^{2+} signals would be fundamental to understand the generation and maintenance of IAS basal tone. Moreover, this endeavor would also be essential to understand the defecation process as the basal tone inhibition is a prerequisite step for defecation under physiological conditions. We do so in this study.

Here, we develop a novel preparation, i.e., precision-cut IAS slice that retains cell arrangement and architecture as *in vivo*. The IAS slices, recorded under light microscopy, generate contractions for hours consisting of phasic and sustained components. Two-photon imaging revealed that IAS SMCs exhibit asynchronized Ca^{2+} oscillations (ACaOs) and synchronized Ca^{2+} oscillations (SCaOs). Quantitative analysis indicates that ACaOs contribute ~25% of sustained contractions, while SCaOs account for 75% of sustained contractions and the entire phasic contractions. Pharmacologic intervention and cell type-specific knockout studies indicate that ACaOs and SCaOs originate in IAS-SMCs, and are independent of ICCs and the nervous system. We further found that ACaOs are due to the opening of RyRs, and SCaOs result from the combined activation of RyRs, TMEM16A, and L-type VDCCs in IAS-SMCs. Finally, nitric oxide (NO), the major neurotransmitter of rectoanal inhibitory reflex or defecation reflex, abolishes both SCaOs and ACaOs to relax IAS fully. Collectively, these results demonstrated that these oscillating Ca^{2+} signals make it possible for the IAS to maintain its tone for a long time without incurring cell damage and that these oscillations are signaling targets of physiological mediators for defecation.

2 | MATERIALS AND METHODS

2.1 | Mice

All animal procedures were approved by the Institutional Animal Care and Use Committees at the University of Massachusetts Medical School (UMMS) (protocol number A1473) in accordance with the National Research Council Publication Guide for the Care and Use of Laboratory Animals and NIH Guide for the Care and Use of Laboratory Animal. Mice were maintained under a standard 12 h light/dark cycle (lights on at 07:00 AM) with food and water ad libitum (room temperature 22±2.0○C). The smooth muscle cell-specific TMEM16A deletion mouse ($TMEM16A^{SMKO}$) was described in our previous study(Zhang et al., 2016). TMEM16A control and $TMEM16A^{SMKO}$ mutant mice were in a mixed C57BL/6 and Sv/129 background. Red-shifted genetically encoded calcium indicators report lines using R-CaMP1.07 were generated by Michael Kotlikoff at Cornell University(Ohkura,

Sasaki, Kobayashi, Ikegaya, & Nakai, 2012) (CHROMus line acta2-RCaMP1.07; Jackson stock #028345). αSMA-hrGFP mice were provided by Alan Fine at Boston University(Paez-Cortez et al., 2013). W/W^V mice were purchased from the Jackson Laboratories (Stock #100410). *c-Kit*^{CreERT2} mice(Klein et al., 2013) were crossed with *Tmem16a*$^{flox/flox}$ mice(Zhang et al., 2016) to generate TMEM16A^{ICCKO} mice. The *Tmem16a* deletion was induced by injecting via i.p. 100 μL corn oil dissolved tamoxifen (10 mg/mL) for 5 consecutive days, and functional tests were conducted 21 days after the last injection.

2.2 | IAS strip force measurement

IAS smooth muscle strips were prepared as described previously(Zhang et al., 2016). Briefly, the anal canal and adjacent rectum (~1.5 cm in length) were quickly removed and transferred to ice-cold and oxygenated Krebs physiological buffer (KPS), which was comprised of (in mM): 118.07 NaCl, 4.69 KCl, 2.52 $CaCl_2$, 1.16 $MgSO_4$, 1.01 NaH_2PO_4, 25 $NaHCO_3$, and 11.10 glucose. Skeletal muscle fibers, mucosal layer, and other extraneous tissues were carefully dissected away and discarded, whereas the anal canal was left intact. The IAS was identified as a thickened circular smooth muscle situated at the lowermost part of the anal canal, and the IAS rings were cut to two halves for experiments.

The IAS strips were transferred to 37°C oxygenated (95% O_2/5% CO_2) KPS, and each end was connected to a force transducer of myograph system (610-M, Danish Myo Technology, Aarhus, Denmark) with 5 mN load. Typically, force declined to 2 mN and then rose again to a sustained level. Strips were equilibrated for 1 hr and then were studied with experimental treatments. To assess the maximal basal tone (which is the sum of maximal sustained force and phasic force minus force when relaxed) of each IAS strip, calcium-free KPS in mM (120.85 NaCl, 4.69 KCl, 1.16 $MgSO_4$, 1.01 NaH_2PO_4, 25 $NaHCO_3$, 1.0 EGTA, and 11.10 glucose) was perfused for a time long enough to reach a stable minimum force (i.e., full relaxation).

2.3 | Precision-cut IAS slice preparation and contraction measurement

The anal canal and adjacent rectum were dissected in Hanks' balanced salt solution (HBSS, Sigma Aldrich), supplemented with 20 mM Hepes buffer and adjusted to pH 7.4 (named as sHBSS). After removing skeletal muscle, mucosal layer, and other tissues, IAS rings were embedded in 5% low melt point agarose gel. After complete gelling at 4°C, the rings were sectioned into ~250 μm thick slices with a compresstome vibratome (VF-300; Precisionary Instruments, Greenville, NC, USA). The consecutive slices were placed, in order, into different wells of a 24-well plate with sHBSS buffer, and examined under a light microscope. The first two slices from the anal verge direction with intact smooth muscle rings were selected for testing such that any contamination from the adjacent rectum was eliminated(Hall, Ward, Cobine, & Keef, 2014). For the contraction measurement, IAS slices with the agarose gel were placed on a cover-glass mounted in custom-made Plexiglas support and held down by a 200 μm nylon mesh with a hole aligned over the IAS slice. A perfusion chamber was created by placing another smaller cover-glass on top of the nylon mesh and sealing the edges with silicone grease. The chamber was perfused by a gravity-fed flow of solution at one end of the chamber and suction at the other end of the chamber. A

custom-built system controlled the application of different solutions, and the flow rate was 500 μl/min. After each treatment, calcium-free HBSS (Modified HBSS without calcium and magnesium, but supplemented with 20 mM Hepes buffer and 0.2 mM EGTA) was perfused for 5 min to determine the intrinsic basal tone of each IAS slice.

IAS slice contraction and relaxation in response to different drugs were monitored with an inverted microscope (Diaphot; Nikon, Tokyo, Japan; or IX71; Olympus, Tokyo, Japan) with a 2× objective. Phase-contrast images were collected at a rate of 0.5 Hz with a CCD camera controlled by custom-programmed software based on Video Savant 4 (IO Industries, Montreal, Canada). The lumen area of the IAS slice was measured as described previously(Tan & Sanderson, 2014). Briefly, images were analyzed with the ImageJ (http://imagesj.nih.gov; NIH, Bethesda, MD, USA). After selecting an appropriate grayscale threshold to distinguish the lumen from the surrounding area, the lumen area of the IAS slice was calculated, with respect to time, by pixel summing. The summed area values were normalized to the initial pre-stimulation value, which was set as 100. Drug-induced percent relaxation was calculated as $(Area_T\text{-}Area_{Ca})/(Area_0\text{-}Area_{Ca})*100$, where $Area_{Ca}$ is the mean value of the last 30 sec in the presence of 1.3 mM Ca^{2+} before any treatment, $Area_T$ the mean lumen area of the last 30 sec during drug treatment and $Area_0$ the mean lumen area of the last 30 sec of 0 calcium solution perfusion.

2.4 | Calcium signal and cell length measurements in IAS slices

IAS slices were loaded with sHBSS containing 20 μM Oregon Green 488 BAPTA-1-AM, 0.1% Pluronic F-127 and 200 μm sulfobromophthalein in the dark at ~31℃ for ~45 min, followed by sHBSS containing 200 μm sulfobromophthalein for an additional 30 min at room temperature to allow the de-esterification of Oregon Green. The Ca^{2+} signals in IAS slices, mounted in the perfusion chamber (described above), were monitored with a custom-built, video-rate scanning two-photon laser microscope as described previously.(Bai & Sanderson, 2006) In brief, a 20× of oil objective (Olympus, Tokyo, Japan, NA 0.80) was used to record fluorescence images. An 800 nm beam from a Ti-sapphire laser (Tsunami, Spectra-Physics, Mountain View, CA) pumped with a 5 W 525 nm diode laser (Millennia, Spectra-Physics) was scanned across the specimen with two oscillating mirrors (X- and Y-scan) through an inverted Olympus IX71FVSF-2 microscope. The emitted fluorescence was separated with a dichroic mirror (670uvdclp, Chroma Technology Corp, Rockingham, VT) and a long pass filter (E600SP-2P, Chroma Technology Corp) positioned immediately below the objective. Emitted fluorescence was detected with a photomultiplier tube (PMT, R5929, Hamamatsu USA, Bridgewater, NJ). Grayscale images (480 × 800 pixels) were recorded at 15 Hz with a frame-grabber (Raven; Bit Flow, Inc). Changes in fluorescence intensity within the images were analyzed by selecting a single SMC. When necessary, a bleach correction was calculated with the bleaching rate observed during a period of 30 s in the presence of extracellular Ca^{2+} before any drug perfusion. Average fluorescence intensities of the entire individual SMC were obtained, frame-by-frame, using the ImageJ software. Fluorescence values were expressed as $(F_t\text{-}F_0)/F_0\times100$, where F_t is the fluorescence intensity at a time point, and F_0 is the mean fluorescence at rest (i.e., without Ca^{2+} oscillation events in the presence of 1.3 mM extracellular Ca^{2+}). Cell lengths were determined using ImageJ to manually trace down the cells' central axis as visualized in the fluorescence image.

2.5 | Immunohistochemical analyses

Anal tissues were isolated, and the skeletal muscle fibers were removed, immediately followed by embedded in Optimal cutting temperature compound (Bio-Tek). Cryosections with a 10-μm thickness were fixed in pre-cooled acetone for 10 min and washed with PBS three times at room temperature. The nonspecific binding of primary antibodies was blocked by incubation with PBST (0.3% Triton in PBS) containing 1% BSA for 1 h. Incubation was carried out overnight at 4°C with a rabbit polyclonal antibody to TMEM16A (ab53212, 1:100; Abcam) and a goat polyclonal antibody against c-Kit (AF332, 1:20; R&D systems). The specificity of these antibodies has been established by vendors and others. After washing in PBS, cells were incubated with an Alexa Fluor 488-conjugated donkey anti-Rabbit IgG H&L (ab150061, 1:500; Abcam) or an Alexa Fluor 594-conjugated rabbit anti-goat IgG (H+L) (A27016, 1:500; Life tech) for 1 h. Negative controls were performed by omitting the primary antibodies. Immunoreactivity was evaluated using a Leica TCS SP5 confocal laser scanning microscope system (Leica Microsystems Inc., Buffalo Grove, IL).

2.6 | Statistical analysis

Data are presented as the mean ± s.e.m. Differences between groups were determined by paired or unpaired Student's t-test for significant differences. The significance levels were indicated as follows: N.S. $P>0.05$, *$P<0.05$, **$P<0.01$, ***$P<0.001$.

3 | RESULTS

3.1 | Mouse IAS Slices Show Sustained Contraction and Phasic Contraction That are Dependent on Extracellular Ca^{2+} and Gap Junction but are Independent of Neurons.

The IAS mainly consists of a band of circular SMCs in mammals and humans. To develop a preparation that potentially retains *in vivo* cell arrangement, we used a vibratome to cut the IAS transversely into 250 μm thickness slices (Fig. 1A; Supplementary Fig. 1A). We first confirmed IAS's smooth muscle structure using a line of the transgenic mouse in which hrGFP is expressed under the control of the α-smooth muscle actin (αSMA) gene promoter(Paez-Cortez et al., 2013). As shown in Supplementary Figure 1B, the precision-cut IAS slice contains a circular ring of GFP positive SMCs, indicating that these IAS slices maintain *in situ* cell architecture. We then assessed the contractile properties of the IAS slices from the first two 250 μm slices from the anal verge direction. This selection criterium ensures the IAS slices used do not contaminate with any adjacent rectum, given that mouse IAS is ~1 mm in width(Hall et al., 2014). After 30 min perfusion with Ca^{2+} buffer at 27°C, these slices developed stable spontaneous phasic contractions (Fig. 1A–1C) that persist for several hours (data not shown). When the extracellular calcium was removed, the phasic contractions gradually faded away and ceased after 2.44 ± 0.45 min (n=6); Interestingly, the precision-cut IAS slices' lumen concurrently enlarged gradually (Fig. 1A–1C) to a stable level. Upon extracellular Ca^{2+} restoration, both phasic contraction and lumen area gradually recovered to the pretreatment level (Fig. 1A–1C, video 1). These results indicate that the IAS slices possess a basal tone, consisting of a sustained contraction component and a phasic contraction component dependent on extracellular Ca^{2+}. This contraction pattern is similar to IAS strips' basal tone under isometric conditions, i.e., a sustained contraction superimposed with rhythmic changes in force (Fig. 1D). As the precision-cut IAS slices

maintain *in situ* cell architecture, these results demonstrate that the IAS slices retain mechanical and physiological characteristics as *in vivo*.

We further characterized IAS slices' contractile responses by treating them with 18β glycyrrhetinic acid, a gap junction inhibitor, and tetrodotoxin (TTX), a voltage-gated Na^+ channel blocker to block action potentials in neurons. We found that 30 μM 18β glycyrrhetinic acid inhibited phasic contractions and decreased the basal tone by 45.92±6.53% (Supplementary Fig. 2; $p<0.01$), but 1 μM TTX generated no effect on phasic contractions and sustained contractions (Supplementary Fig. 3; $p>0.5$). Besides as a gap junction inhibitor, 18β glycyrrhetinic acid has been shown to inhibit L-type Ca^{2+} channels and voltage-gated Na^+ channels (Du et al., 2009). However, the lack of effects of TTX on the contraction (Supplementary Fig. 3) and different inhibitions of phasic contractions by 18β glycyrrhetinic acid and nifedipine (see below) suggest that 18β glycyrrhetinic acid seems not to inhibit L-type Ca^{2+} channels and voltage-gated Na^+ channels to suppress IAS contractions. The data in Supplementary Figs 2 and 3 instead indicate that contractile activities in IAS slices require cell-cell communication via gap junctions but do not involve neurons in IAS, consistent with IAS's properties as revealed in vivo (Rattan, 2005).

3.2 | TMEM16A in ICCs is not Required for the IAS Basal Tone

One hypothesis on the generation of IAS basal tone argues that Ca^{2+}-activated Cl^- channel TMEM16A in ICCs initiates electrical slow waves that propagate to the coupled IAS-SMCs to activate voltage-dependent Ca^{2+} channels (VDCCs), leading to a rise in Ca^{2+} and the tone(C. A. Cobine et al., 2017; Hannigan et al.). However, this hypothesis is based mainly on pharmacological and electrophysiological studies. Hence we examined its validity by genetically deleting TMEM16A in ICCs (i.e., $TMEM16A^{ICCKO}$ mice) by crossing *Tmem16a*$^{fl/fl}$ mice with *c-Kit*^{CreERT2} mice. We first confirmed the deletion of TMEM16A in ICCs by studying the impairments in the gastric antrum contraction, a phenotype reported by Hwang *et al*. in a line of $TMEM16A^{ICCKO}$ mice(Hwang et al., 2019) that was generated with a similar approach as in the current study. We found that, compared to isogenic control mice, in gastric antrum from $TMEM16A^{ICCKO}$ mice, the amplitude of phasic contraction was decreased from 1.05±0.13mN to 0.4±0.10mN, while there was no change in its frequency (4.65±0.24min^{-1} in control mice vs. 4.7±0.36min^{-1} in $TMEM16A^{ICCKO}$ mice) (Supplementary Fig. 4). These results are similar to those revealed by Hwang *et al*(Hwang et al., 2019). Having confirmed the role of TMEM16A in gastric antrum using $TMEM16A^{ICCKO}$ mice, we went on to assess its role in IAS. As shown in Fig. 2A, TMEM16A is expressed in c-Kit positive cells in IAS from control mice but not in those from $TMEM16A^{ICCKO}$ mice. However, no changes were detected in contractile activity between IAS slices from control mice and $TMEM16A^{ICCKO}$ mice (Fig. 2B and 2C). To further test the ICC hypothesis, we assessed the contractile activity of IAS slices from c-kit mutant W/W^V mice whose ICCs are severely deficient(de Lorijn et al., 2005). We found no difference in the sustained contractions and phasic contractions between IAS slices from ICC deficient mice and wild type controls (Fig. 2B and 2C). These findings strongly argue that TMEM16A in ICCs is not necessary to generate IAS' sustained contraction or phasic contraction, hence the basal tone.

3.3 | The RyR-TMEM16A-VDCC Axis in IAS-SMCs is Required for the IAS Basal Tone

Our previous study showed that the RyR-TMEM16A-VDCC signaling module in IAS-SMCs plays an essential role in setting the mouse IAS's basal tone(Zhang et al., 2016). Given IAS slices' novelty, we decided to confirm whether these channels work under a more physiological setting. The phasic contractions of IAS slices were entirely blocked by RyR inhibitor ryanodine (Fig. 3A and 3D), and by specific L-type VDCC blocker nifedipine (19.25±1.25 min^{-1} before nifedipine treated v.s. 1.75±0.85 min^{-1} after nifedipine) (Fig. 3B and 3E). The sustained contraction was also suppressed by 85.49±2.11% and 66.48±4.85% by ryanodine and nifedipine (Fig. 3F). To genetically test this model, we determined the sustained contraction and phasic contraction in IAS slices from $TMEM16A^{SMKO}$ mice (i.e., TMEM16A in SMCs was specifically deleted). We found that the sustained contraction in IAS slices from these knockout mice was reduced by ~75% (i.e., sustained contraction was 12.10±2.90% in knockout mice v.s. 48.73±7.12% in control mice), and phasic contractions were eliminated (22.17±1.54 min^{-1} in control mice vs. 0.56±0.24 min^{-1} in $TMEM16A^{SMKO}$ mice) (Fig. 3C and 3G, Video 2 and 3.). These results, therefore, indicate that RyRs, L-type VDCCs and TMEM16A are necessary for not only the generation of sustained and phasic contractions but also their maintenance in mouse IAS.

3.4 | IAS-SMCs Exhibit Synchronous Ca^{2+} Oscillations (SCaOs) and Asynchronous Ca^{2+} Oscillations (ACaOs).

Given (1) the different activation and inactivation properties of RyR, L-type VDCCs and TMEM16A, and (2) the central role of Ca^{2+} in controlling smooth muscle contractility, we hypothesized that Ca^{2+} signals which underlie the sustained contraction and phasic contraction in IAS slices must differ in frequency and/or amplitude. To search for these Ca^{2+} signals, we loaded IAS slices with Ca^{2+} indicator Oregon Green 488 BAPTA-1 AM (20 μM) and performed real-time lapse imaging under two-photon microscopy. In the presence of extracellular Ca^{2+}, IAS-SMCs exhibit two types of spontaneous calcium oscillations: one is synchronized Ca^{2+} oscillations (SCaOs) (Fig. 4A and video 4), in which a group of SMCs display rhythmic rises in $[Ca^{2+}]i$ at the same time, and the other is asynchronized Ca^{2+} oscillations (ACaOs) (Fig. 4B and video 5), in which each cell displays repetitive increases in $[Ca^{2+}]i$ at random. The ΔF/F0 amplitude of SCaOs was 79.41±3.10% and ACaOs 106.67±11.54%, while the frequency of SCaOs in the IAS was 23.71±1.87 min-1 and ACaOs 16.14±1.08 min-1. When the standard Ca^{2+} buffer was replaced with a Ca^{2+} free buffer, both SCaOs and ACaOs were decreased time-dependently and ceased in about 2 min and 4 min, respectively (Fig. 4C–4F). SCaOs propagated along the long axis of IAS muscle bundle, which can be different from, and independent of, the flow orientation of the solution perfusion. This argues against the role of signaling molecules secreted via a paracrine or autocrine process in the generation of SCaOs. (For in vitro experiments as in this study, any involvement of endocrine mechanisms can also be ruled out.) We confirmed that IAS-SMCs produced these Ca^{2+} signals because the IAS slices from mice whose SMCs genetically express red fluorescent Ca^{2+} indicator RCaMP1.07 produced SCaOs and ACaOs with the similar amplitudes and frequencies (supplementary Fig. 5, videos 6 and 7). These results suggest that two Ca^{2+} signals could underlie the basal tone, as observed in Figure 1.

To examine the involvement of gap junctions and nerves on the genesis of SCaOs and ACaOs, we treated IAS slices with 30 μM 18β glycyrrhetinic acid and 1 μM TTX. We found that 18β glycyrrhetinic acid inhibited both the amplitude and frequency of SCaOs, but showed no influence on those parameters of ACaOs (Supplementary Fig. 6). However, TTX produced no effect on the activity of both SCaOs and ACaOs (Supplementary Fig. 7). In conjunction with the observation that the SCaO propagation direction is independent of the solution perfusion, these results reinforce the conclusion that both SCaOs and ACaOs originate from IAS-SMCs and are not mediated by neurotransmission or signaling molecule releases via paracrine or autocrine processes.

3.5 | ACaOs and SCaOs Exert Different Roles in IAS-SMC Sustained Contraction and Shortening.

To examine the role of SCaOs in IAS-SMC sustained contraction, we compared the length of cells in the IAS regions with SCaOs when extracellular Ca^{2+} was present or absent. The length in the presence of extracellular Ca^{2+} was measured when SCaOs returned to the basal level, while that in the absence of extracellular Ca^{2+} was when Ca^{2+} free medium had been perfused for 5 min (Fig. 4A). Figure 5A shows that the removal of extracellular Ca^{2+} increased the cell length (122.39±6.32 μm in the presence of extracellular Ca^{2+} and 148.53±7.77μm in its absence).

To determine whether ACaOs contribute to IAS-SMC sustained contraction, we examined the regions without SCaOs in the IAS slices. We compared between IAS slices in medium with and without extracellular Ca^{2+}. The end to end cell length in the presence of extracellular Ca^{2+} was measured at the time when ACaOs had returned to the basal level. The length in the absence of extracellular Ca^{2+} was measured when Ca^{2+} free medium had been perfused for 5 min (Fig. 4B). As shown in Fig. 5D, the cell length was 148.50±7.60 μm in the presence of extracellular Ca^{2+} and 167.75±7.98 μm in its absence.

To assess whether SCaOs or ACaOs could induce dynamic changes in IAS-SMC length or shortening, we measured the cell length changes associated with these Ca^{2+} events. We detected whenever there was a SCaO event in a group of IAS-SMCs, these cells contracted, and the same repetitive SCaO event caused the contraction in the same direction and distance (Video 4). On average, SCaOs shortened the end to end length of the IAS-SMCs by 28.74±2.26% (Fig. 5B and 5C). However, no association between cell length changes and the occurrence of ACaOs (Fig. 5E). These data indicate that both SCaOs and ACaOs contribute to the sustained contraction of IAS-SMCs, while only SCaOs produce rhythmic shortening.

3.5 | Molecular Basis of SCaOs

To uncover the molecular basis of SCaOs, we treated IAS slices with inhibitors of RyRs and L-type VDCCs. Ryanodine entirely blocked SCaOs (Fig. 6A, 6D, and 6E) and increased the ISM-SMC length by 17.54±2.79% (Fig. 6G), while nifedipine abolished SCaOs (Fig. 6B, 6D and 6E), and increased the length by 14.36±1.98% (Fig. 6G). The length change by ryanodine was comparable to, but nifedipine was less than that by removing extracellular Ca^{2+} (22.34±3.30%) (Fig. 6G). To determine the role of TMEM16A in SCaOs and IAS-

SMC shortening, we compared Ca^{2+} signals and their associated cell shortening between IAS slices from isogenic control mice and $TMEM16A^{SMKO}$ mice. We found that in control, SCaOs had an amplitude of 82.25±7.47% and a frequency of 22.56±1.86 min^{-1} (Fig. 6C and 6F), and each SCaO caused ISM-SMC shortening by 27.58±3.31% (n= 30 cells from 3 mice). Strikingly, we could not detect any SCaOs in the IAS slices without TMEM16A (Fig. 6C and 6F). These results indicate that RyRs, L-type VDCCs, and TMEM16A are required for SCaOs and their resultant cell shortening in the IAS.

3.6 | Molecular Basis of ACaOs

IAS-SMCs from $TMEM16A^{SMKO}$ mice do not generate SCaOs (see above). However, these cells generate ACaOs, just as in the isogenic control cells (Fig. 6C, 4B, 4E, and 4F; amplitude: 105.88±4.41% in $TMEM16^{SMKO}$cells vs. 106.67±11.54% in wild type cells; frequency: 15.23±0.93 min^{-1} in $TMEM16A^{SMKO}$ cells vs. 16.14±1.08 min^{-1} in wild type cells). This unique feature in IAS-SMCs from $TMEM16A^{SMKO}$ mice allows us to study the molecular basis of ACaOs and their role in cell shortening without interference from SCaOs. In IAS slices from $TMEM16A^{SMKO}$ mice, Ca^{2+} free solution entirely blocked ACaOs as in wild type mice as shown in Fig. 4 (data not shown) and increased the cell length by 13.58±1.44% (Fig. 7E). Similarly, ryanodine blocked ACaOs (Fig. 7A, C, and 7D) and lengthened the cells by 11.74±1.28% (Fig. 7E). However, nifedipine produced no effect on ACaO frequency and cell length (Fig. 7C, 7D, and 7E). These results demonstrate that RyRs underlie ACaOs, which can contribute to the sustained contraction of IAS-SMCs. Considering that the sustained contraction of IAS slices in $TMEM16A^{SMKO}$ mice was decreased by ~75% (Fig. 3C and 3G), it is estimated that ACaOs could contribute ~25% of the sustained contraction in these slices.

3.7 | Physiological Neurotransmitter Nitrate Oxide Blocks SCaOs and ACaOs to Relax IAS

IAS's transient relaxation in response to rectal distention, i.e., the rectoanal inhibitory reflex (RAIR), plays a vital role in the defecation reflex. Nitric oxide (NO) is the primary physiological neurotransmitter for RAIR(Rattan & Singh, 2011b). We, therefore, assessed whether NO exerts any effects on SCaOs and ACaOs. Figure 8A shows that NO donor sodium nitroprusside (SNP, 1 μM) completely abrogated SCaOs and ACaOs (Fig. 8A, 8B, 8C, and 8E), i.e., both frequencies of SCaO and ACaO were 100% inhibited (Fig. 8D and 8F) upon activation for 5 min. The inhibition in SCaOs and ACaOs was associated with an increase in the cell length, i.e., 20.57±2.23% and 15.95±2.16%, respectively, after 5 min perfusion (Fig. 8G). These effects were not due to the toxicity of SNP because the washout of SNP led to the partial recovery of Ca^{2+} signals (Fig. 8A and 8B). To link these effects of SNP to the IAS tissue function, we treated the IAS slices with the same SNP concentration. We found that SNP at 1 μM blocked both phasic contractions and sustained contractions to the same maximal level, as seen in the absence of Ca^{2+} (Fig. 8H–8J). These data indicate that the RIAR mediator NO blocks SCaOs and ACaOs, leading to IAS full relaxation.

4 | DISCUSSION

In this study, we uncover a cellular mechanism underlying IAS's basal tone, as depicted in Figure 9. With a novel PC-IAS preparation and two-photon microscopy, we observed that

the IAS generates sustained and phasic contraction and produces SCaOs and ACaOs. Using pharmacological and cell-specific gene knockout techniques, we established that both SCaOs and ACaOs originate from IAS-SMCs. Furthermore, we determined that SCaOs result from the combined activation of RyR-TMEM16A-VDCC and are solely responsible for phasic contraction as well as account for ~75% of the sustained contraction, and ACaOs are mediated by RyRs and contribute to ~25% of the sustained contraction. Finally, we discovered that physiological neurotransmitter NO abolishes both SCaOs and ACaOs, and fully relaxes IAS.

4.1 | PC-IAS Slices Maintain IAS's Physiologically Relevant Contractile Activity

Physiological responses are context-dependent. Precision-cut tissue slices have been demonstrated as a choice to study physiology in various tissues because these tissue slices preserve the same complex cell architecture and maintain the local cell-cell and cell-matrix contacts seen *in vivo*(Krumdieck, dos Santos, & Ho, 1980; Li, de Graaf, & Groothuis, 2016). Another advantage for tissue slices is that their thickness is well suited for advanced imaging modalities such as two-photon microscopy(Benninger & Piston, 2013). For these reasons, we developed the first, to our knowledge, precision-cut IAS preparation. Several features of this preparation demonstrate its uniqueness and suitability for studying contractile responses and Ca^{2+} signaling in IAS. First, IAS slices maintain their phasic and sustained contraction for several hours, reflecting the sphincter nature of IAS *in vivo*. Second, because of the preservation of their original cellular organization, IAS slices reveal more physiological responses than IAS strips studied under the often-used isometric configuration. At first, it came as a surprise that no phasic contraction was observed in the IAS slices from $TMEM16A^{SMKO}$ mice because under isometric conditions, the IAS strips from the same mice generated phasic contractions (although at a much lower frequency, supplementary Fig. 9A). However, the strips' phasic contractions are most likely due to the imposed stretch or load under the isometric condition because they were not induced (Supplementary Fig. 9B) when no stretch and load (i.e., nature curving state) were applied to the IAS strips. And third, in conjunction with two-photon fluorescence microscopy, Ca^{2+} signals and cell length in the IAS slices can be detected and quantified at the cellular and subcellular levels. This capability allows one to study Ca^{2+} signals and their function at both single and multiple cell resolutions. Indeed, we detected unique Ca^{2+} signals that were not seen in isolated single IAS-SMCs in our previous study(Zhang et al., 2016). For example, we previously found that global Ca^{2+} rises mediated by Ca^{2+} sparks, the Ca^{2+} release events due to the opening of a small number of RyRs(Nelson et al., 1995; ZhuGe, Sims, Tuft, Fogarty, & Walsh, 1998), can shorten IAS-SMCs. Nevertheless, in this study, we found that Ca^{2+} rise from individual SMCs (i.e., ACaOs) can contribute only about 25% of sustained contraction in IAS slices. Therefore the IAS preparation developed in this study possesses the advantages needed to uncover the characteristics of IAS basal tone.

4.2 | SCaOs and ACaOs Generated by IAS-SMCs Differentially Contribute to IAS Basal Tone

With novel PC-IAS slices, we have revealed the Ca^{2+} signals underlying IAS basal tone. Previous studies, including ours, have suggested that a Ca^{2+} increase is necessary for generating the basal tone(Zhang et al., 2016). What remained unclear was the nature of the

Ca^{2+} signals. Finding these signals is essential in understanding IAS physiology because IAS maintains a tone for a substantial time, but a prolonged increase in cytosolic Ca^{2+} concentration would damage cells and even cause them to die(Cerella et al., 2010; Zhivotovsky & Orrenius, 2011). With two-photon imaging of IAS slices, we have identified and decoded these Ca^{2+} signals. We found that IAS-SMCs continuously generate two types of oscillating Ca^{2+} signals, SCaOs and ACaOs. We further found that the deletion of TMEM16A in IAS-SMCs abolishes SCaOs without interference with ACaOs. This striking effect offered us a unique opportunity to establish the contribution of SCaOs and ACaOs to the two components of basal tone in the IAS. Due to their asynchronous nature, ACaOs may not impact the basal tone as much as one would predict. However, after TMEM16A deletion in SMCs, IAS slices maintain ~25% of the sustained contraction compared to the isogenic control. The remaining contraction and ACaOs can be abolished by ryanodine. On the other hand, $TMEM16A^{SMKO}$ mice reveal that SCaOs are fully responsible for phasic contraction in IAS and contribute to ~75% of sustained contraction. The causal effect on phasic contraction by SCaOs is evident from our data, but the effect of SCaOs on the sustained contraction may not be as direct. In theory, a downstream mechanism, for example, myosin light chain phosphorylation and dephosphorylation(Gao et al., 2016; Gao et al., 2013; Somlyo & Somlyo, 1994), or the latch bridge (i.e., when the myosin cross-bridge remains attached to an actin filament after myosin light chain kinase and myosin light chain phosphatase are deactivated)(Hai & Murphy, 1988; Murphy & Rembold, 2005), may convert the transient SCaO signals to a prolonged signal to maintain IAS-SMC contraction. Whether this is true or not, the oscillating character of SCaOs and ACaOs satisfies the need for a rise in cytosolic Ca^{2+} to maintain the ISA tone while avoiding the prolonged and constant rise in cytosolic Ca^{2+}, which would damage IAS-SMCs.

Generally speaking, Ca^{2+} oscillations can be initiated by a cytosolic oscillator (i.e., calcium release from internal Ca^{2+} stores) or by a membrane oscillator (e.g., the opening and closing of VDCCs in the plasma membrane)(Berridge & Galione, 1988; Imtiaz, von der Weid, & van Helden, 2010). We found that ryanodine can entirely block ACaOs and SCaOs, but while nifedipine can abolish SCaOs, it exerts no effect on ACaOs. Therefore, ACaOs are governed by a cytosolic oscillator, i.e., RyRs, which spontaneously open and close in the sarcoplasmic reticulum, while both cytosolic oscillators and membrane oscillators influence SCaOs.

Studies have revealed that cytosolic oscillators via Ca^{2+} diffusion can generate Ca^{2+} waves with a low propagating velocity, but membrane oscillators via electrical coupling can generate highly coordinated long-range Ca^{2+} waves(Berridge & Galione, 1988; Imtiaz et al., 2010; van Helden & Imtiaz, 2003). This study reveals that SCaOs can propagate to a much larger area at a higher velocity than ACaOs. The involvement of both the cytosolic oscillator and membrane oscillator for SCaOs raises an intriguing question of how these two oscillators are coupled. In guinea-pig gastric pylorus, Van Helden *et al.* demonstrated that two factors substantially enhance the coupling to generate synchronicity over a wide separated space(van Helden & Imtiaz, 2003). First, a Ca^{2+} release from internal Ca^{2+} stores depolarizes the plasma membrane, and second, the depolarization enhances additional Ca^{2+} release from the store. The machinery composed of RyRs, L-type VDCCs, and TMEM16A in IAS-SMCs satisfies these requirements to yield SCaOs as follows. A SMC is a local

cytosolic oscillator capable of releasing Ca^{2+} from internal Ca^{2+} stores via RyRs. The rise in Ca^{2+}, in turn, activates TMEM16A to depolarize membranes followed by electrical propagation to the adjacent SMCs via gap junctions. Finally, the depolarization activates L-type VDCC to allow Ca^{2+} influx, which activates RyRs and generates Ca^{2+}-induced Ca^{2+} release from the internal Ca^{2+} stores.

The different molecular bases of ACaOs and SCaOs suggest that there are at least two subpopulations of SMCs in mouse IAS. One expresses RyRs, but lacks TMEM16A and/or L-type VDCCs, to generate only ACaOs, and the other expresses RyRs, TMEM16A, and L-type VDCCs to generate SCaOs. This possibility is supported by our previous study showing that TMEM16A distributes in the IAS-SMCs adjacent to the submucosal space of the distal end of anorectum, and not all the IAS-SMCs show Cl_{Ca} currents(Zhang et al., 2016). It would be interesting to determine the distribution patterns of RyRs and L-type VDCCs in IAS-SMCs and, more importantly, each IAS-SMC subpopulation's physiological roles in IAS basal tone.

4.3 | TMEM16A in ICCs Plays a Marginal Role in Generating Ca^{2+} Signals and Basal Tone in IAS

The gastrointestinal system's motility involves coordinating several cell types, including neurons, SMCs, and ICCs. ICCs are thought to serve as electrical pacemakers, and TMEM16A in these cells is considered the pacemaking channel(Sanders, Kito, Hwang, & Ward, 2016). Recent ICC-specific TMEM16A deletion studies have substantially strengthened this critical idea(Hwang et al., 2019; Malysz et al., 2017). However, these recent studies also revealed that the pacemaking role of TMEM16A might only operate in specific segments of the gastrointestinal system. For example, the ICC TMEM16A deletion causes a dramatic decrease or loss of gastric slow waves, disrupts gastric contractile patterns, and reduces the gastric emptying rate. However, the same deletion does not affect any slow-wave parameters and the amplitude and frequency of contractions in the small intestine(Hwang et al., 2019). This lacking role of TMEM16A in the small intestine can not be attributed to its expression level or the inefficiency of the Cre-induced deletion in this gastrointestinal region(Hwang et al., 2019). Given the power of cell-specific gene knockout technology, in this study, we generated a line of TMEM16A knockout mice in which TMEM16A is deleted specifically in ICCs to determine its role in the Ca^{2+} signaling and basal tone of IAS. Strikingly, we found that both phasic and sustained contractions of $TMEM16A^{ICCKO}$ IAS slices are not different from those from the isogenic control mice. We validated the effectiveness of the TMEM16A deletion in ICCs as contractions in gastric antrum from the same mice were severely suppressed, which is similar to the finding in another $TMEM16A^{ICCKO}$ mouse line(Hwang et al., 2019). In contrast, when TMEM16A in SMCs is deleted, IAS-SMCs failed to generate SCaOs and produce less than 25% of sustained contraction, indicating that TMEM16A in IAS-SMCs plays a critical role in the generation of basal tone in IAS. Our results in $TMEM16A^{ICCKO}$ mice are consistent with the results from ICC-deficient W/W^V mice. We found that Ca^{2+} signals (data not shown) and two forms of contractions in W/W^V mice are also not different from wild type mice. These results are in line with studies showing that slow waves are not impaired in W/W^V mice(de Lorijn et al., 2005; Duffy, Cobine, & Keef, 2012). Hence it is reasonable to

conclude that TMEM16A in IAS-ICCs may play, at most, a minor role in generating Ca^{2+} signals in IAS-SMCs and phasic and sustained contraction in the IAS.

4.4 | SCaOs and ACaOs are the Target of Neurotransmitter NO, which is Essential for Defecation.

The IAS tone is required to maintain fecal continence. On the other hand, a decrease in tone is necessary for evacuation of fecal contents. Physiologically feces accumulation in the rectum activates inhibitory motor neurons, which in turn relax the IAS leading to defecation, a process called RAIR(Rao, 2004; A. P. Zbar et al., 1998). It is well established that NO is the primary neurotransmitter of these inhibitory motor neurons in the RAIR(Rattan, Regan, Patel, & De Godoy, 2005; Rattan & Singh, 2011b). However, the mechanisms by which NO relaxes IAS remain to be fully understood. In this study, we found NO can altogether abolish both SCaOs and ACaOs. These effects exert a significant impact on IAS tone because NO also fully inhibits phasic and sustained contractions of IAS slices. These results indicate the importance of SCaOs and ACaOs in anorectal physiological functions.

How NO inhibits SCaOs and ACaOs warrants additional studies. Nevertheless, we can propose at least three potential mechanisms. First, as RyRs mediate SCaOs and ACaOs, it is plausible that NO inhibits RyRs directly or indirectly in IAS-SMCs. In striated muscle and neurons, NO has a direct effect on RyRs via covalent S-nitrosylation, leading to an increase in RyR open probability(Stamler, Sun, & Hess, 2008; Sun et al., 2008). In smooth muscle, although NO produces relaxation via a cGMP-dependent mechanism, the effect of NO on RyRs can be inhibitory or stimulatory. In airway smooth muscle, NO inhibits RyR-mediated global Ca^{2+} release(Kannan, Prakash, Johnson, & Sieck, 1997), while in cerebral arterial smooth muscle, NO increases RyR-mediated Ca^{2+} sparks(Mandala, Heppner, Bonev, & Nelson, 2007). It is noteworthy that the expression of ion channels activated by RyR-mediated Ca^{2+} signals is different between these two smooth muscles. In airway smooth muscle cells, Ca^{2+} release from RyRs activates large-conductance Ca^{2+}-activated K^+ (BK) channels and TMEM16A Ca^{2+}-activated Cl^- channels(Bao et al., 2008; ZhuGe et al., 1998). However, in cerebral arterial smooth muscle cells, Ca^{2+} sparks activate only BK channels(Brenner et al., 2000; Nelson et al., 1995). We previously found that a RyR-mediated Ca^{2+} rise opens Ca^{2+}-activated Cl^- channel in IAS-SMCs(Zhang et al., 2016). So it is likely that NO exhibits an inhibitory effect on RyRs in smooth muscle cells that express TMEM16A. Second, NO could inhibit L-type VDCCs to block SCaOs in IAS-SMCs. This is highly likely because several studies, including one in IAS-SMCs, have demonstrated that NO can reduce the L-type VDCC channel activity via cGMP dependent and independent mechanisms(C. A. Cobine et al., 2014; Quignard et al., 1997; Sharma, Bhattarai, Hwang, & Han, 2013). And finally, the effect of NO on TMEM16A could be mediated through inhibition of RyRs and L-type VDCCs or by direct modulation of the channel itself. For the former, it would be simply due to the fact that Ca^{2+} activates TMEM16A so a decrease in Ca^{2+} after RyR or L-type VDCC inhibition would decrease the activity of TMEM16A. For the latter, NO may inhibit TMEM16A via protein kinase G to block SCaOs in IAS-SMCs as TMEM16A can interact with many proteins(Perez-Cornejo et al., 2012; Yu, Jiang, Cui, Tajkhorshid, & Hartzell, 2019) and NO inhibits Ca^{2+}-activated Cl^- channel activities in

several smooth muscles(Craven, Sergeant, Hollywood, McHale, & Thornbury, 2004; Waniishi et al., 1998).

NO abolishing SCaOs and ACaOs to relax IAS fully could be an essential mechanism of the RAIR. This raises the possibility that co-transmitters (e.g., ATP) of NO in the RAIR likely regulate these Ca^{2+} signals' activity to relax IAS partially(Rattan & Singh, 2011b). Given that mechanical tension can modulate IAS's contractile response, the tension may also alter the activity of SCaOs and ACaOs. Thus the discovery of SCaOs and ACaOs and their roles in the sustained contraction and phasic contraction in IAS suggests that these Ca^{2+} signals may serve as the contractile signaling system that allows stool to pass the anus in a precisely controlled manner.

In summary, with a novel IAS preparation, cell-specific gene knockout techniques, and two-photon microscopy, we have unveiled that two oscillating Ca^{2+} signals (SCaOs and ACaOs) generated by the interplay of RyRs, L-type VDCCs and TMEM16A or the opening of RyRs alone in the IAS-SMCs can generate the persistent basal tone in IAS. This tone is composed of two components, a sustained component and a phasic component (at ~20/min). SCaOs are solely responsible for phasic contraction and ~75% of the sustained contraction, while ACaOs only contribute to ~25% of the sustained contraction. Besides, these Ca^{2+} signals and the resultant basal tone are not dependent on TMEM16A in ICCs or the neurons in IAS. Finally, neurotransmitter NO targets these Ca^{2+} signals to relax IAS fully. As NO is the central mediator of the RAIR, the mechanism revealed here deepens our understanding of normal defecation and fecal continence.

Supplementary Material

Refer to Web version on PubMed Central for supplementary material.

ACKNOWLEDGEMENTS

This work was supported by the National Institute of Health (RO1DR098586 to R.Z.) and by the funding from the University of Massachusetts Medical School to R.Z. We would like to thank Dr. Michael Kotlikoff for providing CHROMus line acta2-RCaMP1.07 mice, and Dr. Allan Fine for αSMA-hrGFP mice.

References

Athamneh K, Alneyadi A, Alsamri H, Alrashedi A, Palakott A, El-Tarabily KA, . . . Iratni R. (2020). Origanum majorana Essential Oil Triggers p38 MAPK-Mediated Protective Autophagy, Apoptosis, and Caspase-Dependent Cleavage of P70S6K in Colorectal Cancer Cells. Biomolecules, 10(3). doi:10.3390/biom10030412

Bai Y, & Sanderson MJ (2006). Modulation of the Ca2+ sensitivity of airway smooth muscle cells in murine lung slices. Am J Physiol Lung Cell Mol Physiol, 291(2), L208–221. doi:10.1152/ajplung.00494.2005 [PubMed: 16461427]

Bao R, Lifshitz LM, Tuft RA, Bellve K, Fogarty KE, & ZhuGe R. (2008). A close association of RyRs with highly dense clusters of Ca2+-activated Cl- channels underlies the activation of STICs by Ca2+ sparks in mouse airway smooth muscle. J Gen Physiol, 132(1), 145–160. doi:10.1085/jgp.200709933 [PubMed: 18591421]

Benninger RK, & Piston DW (2013). Two-photon excitation microscopy for the study of living cells and tissues. Curr Protoc Cell Biol, Chapter 4, Unit 4.11.11–24. doi:10.1002/0471143030.cb0411s59

Berridge MJ, & Galione A. (1988). Cytosolic calcium oscillators. Faseb j, 2(15), 3074–3082. doi:10.1096/fasebj.2.15.2847949 [PubMed: 2847949]

Bharucha AE (2004). Outcome measures for fecal incontinence: anorectal structure and function. Gastroenterology, 126(1 Suppl 1), S90–98. doi:10.1053/j.gastro.2003.10.014 [PubMed: 14978644]

Brenner R, Perez GJ, Bonev AD, Eckman DM, Kosek JC, Wiler SW, . . . Aldrich RW (2000). Vasoregulation by the beta1 subunit of the calcium-activated potassium channel. Nature, 407(6806), 870–876. doi:10.1038/35038011 [PubMed: 11057658]

Cerella C, Diederich M, & Ghibelli L. (2010). The dual role of calcium as messenger and stressor in cell damage, death, and survival. Int J Cell Biol, 2010, 546163. doi:10.1155/2010/546163 [PubMed: 20300548]

Cobine CA-O, Hannigan KI, McMahon M, Ni Bhraonain EP, Baker SA-O, & Keef KD Rhythmic calcium transients in smooth muscle cells of the mouse internal anal sphincter. (1365–2982 (Electronic)).

Cobine CA, Hannah EE, Zhu MH, Lyle HE, Rock JR, Sanders KM, . . . Keef KD (2017). ANO1 in intramuscular interstitial cells of Cajal plays a key role in the generation of slow waves and tone in the internal anal sphincter. J Physiol, 595(6), 2021–2041. doi:10.1113/jp273618 [PubMed: 28054347]

Cobine CA, Sotherton AG, Peri LE, Sanders KM, Ward SM, & Keef KD (2014). Nitrergic neuromuscular transmission in the mouse internal anal sphincter is accomplished by multiple pathways and postjunctional effector cells. Am J Physiol Gastrointest Liver Physiol, 307(11), G1057–1072. doi:10.1152/ajpgi.00331.2014 [PubMed: 25301187]

Craven M, Sergeant GP, Hollywood MA, McHale NG, & Thornbury KD (2004). Modulation of spontaneous Ca2+-activated Cl- currents in the rabbit corpus cavernosum by the nitric oxide-cGMP pathway. J Physiol, 556(Pt 2), 495–506. doi:10.1113/jphysiol.2003.058628 [PubMed: 14766939]

de Lorijn F, de Jonge WJ, Wedel T, Vanderwinden JM, Benninga MA, & Boeckxstaens GE (2005). Interstitial cells of Cajal are involved in the afferent limb of the rectoanal inhibitory reflex. Gut, 54(8), 1107–1113. doi:10.1136/gut.2004.051045 [PubMed: 16009682]

Du Y, Zhang S Fau - Wu H, Wu H Fau - Zou A, Zou A Fau - Lei M, Lei M Fau - Cheng L, Cheng L Fau - Liao Y, & Liao Y. (2009). Glycyrretinic acid blocks cardiac sodium channels expressed in Xenopus oocytes. J Ethnopharmacol(1872–7573 (Electronic)).

Duffy AM, Cobine CA, & Keef KD (2012). Changes in neuromuscular transmission in the W/W(v) mouse internal anal sphincter. Neurogastroenterol Motil, 24(1), e41–55. doi:10.1111/j.1365-2982.2011.01806.x [PubMed: 22074497]

Foxx-Orenstein AE, Umar SB, & Crowell MD Common anorectal disorders. (1554–7914 (Print)).

Gao N, Chang AN, He W, Chen CP, Qiao YN, Zhu M, . . . Stull JT (2016). Physiological signalling to myosin phosphatase targeting subunit-1 phosphorylation in ileal smooth muscle. J Physiol, 594(12), 3209–3225. doi:10.1113/JP271703 [PubMed: 26847850]

Gao N, Huang J, He W, Zhu M, Kamm KE, & Stull JT (2013). Signaling through myosin light chain kinase in smooth muscles. J Biol Chem, 288(11), 7596–7605. doi:10.1074/jbc.M112.427112 [PubMed: 23362260]

Guillaume A, Salem AE, Garcia P, & Chander Roland B. (2017). Pathophysiology and Therapeutic Options for Fecal Incontinence. J Clin Gastroenterol, 51(4), 324–330. doi:10.1097/mcg.0000000000000797 [PubMed: 28267690]

Hai CM, & Murphy RA (1988). Cross-bridge phosphorylation and regulation of latch state in smooth muscle. Am J Physiol, 254(1 Pt 1), C99–106. doi:10.1152/ajpcell.1988.254.1.C99 [PubMed: 3337223]

Hall KA, Ward SM, Cobine CA, & Keef KD (2014). Spatial organization and coordination of slow waves in the mouse anorectum. J Physiol, 592(17), 3813–3829. doi:10.1113/jphysiol.2014.272542 [PubMed: 24951622]

Hannigan KI, Bossey AP, Foulkes HJL, Drumm BT, Baker SA, Ward SM, . . . Cobine CA A novel intramuscular Interstitial Cell of Cajal is a candidate for generating pacemaker activity in the mouse internal anal sphincter. (2045–2322 (Electronic)).

Hwang SJ, Pardo DM, Zheng H, Bayguinov Y, Blair PJ, Fortune-Grant R, . . . Ward SM (2019). Differential sensitivity of gastric and small intestinal muscles to inducible knockdown of anoctamin 1 and the effects on gastrointestinal motility. J Physiol, 597(9), 2337–2360. doi:10.1113/jp277335 [PubMed: 30843201]

Imtiaz MS, von der Weid PY, & van Helden DF (2010). Synchronization of Ca2+ oscillations: a coupled oscillator-based mechanism in smooth muscle. Febs j, 277(2), 278–285. doi:10.1111/j.1742-4658.2009.07437.x [PubMed: 19895582]

Kannan MS, Prakash YS, Johnson DE, & Sieck GC (1997). Nitric oxide inhibits calcium release from sarcoplasmic reticulum of porcine tracheal smooth muscle cells. Am J Physiol, 272(1 Pt 1), L1–7. doi:10.1152/ajplung.1997.272.1.L1 [PubMed: 9038895]

Klein S, Seidler B, Kettenberger A, Sibaev A, Rohn M, Feil R, . . . Saur D. (2013). Interstitial cells of Cajal integrate excitatory and inhibitory neurotransmission with intestinal slow-wave activity. Nat Commun, 4, 1630. doi:10.1038/ncomms2626 [PubMed: 23535651]

Krumdieck CL, dos Santos JE, & Ho KJ (1980). A new instrument for the rapid preparation of tissue slices. Anal Biochem, 104(1), 118–123. doi:10.1016/0003-2697(80)90284-5 [PubMed: 6770714]

Kumar L, & Emmanuel A. (2017). Internal anal sphincter: Clinical perspective. Surgeon, 15(4), 211–226. doi:10.1016/j.surge.2016.10.003 [PubMed: 27881288]

Lee YY (2014). What's New in the Toolbox for Constipation and Fecal Incontinence? Front Med (Lausanne), 1, 5. doi:10.3389/fmed.2014.00005 [PubMed: 25705618]

Li M, de Graaf IA, & Groothuis GM (2016). Precision-cut intestinal slices: alternative model for drug transport, metabolism, and toxicology research. Expert Opin Drug Metab Toxicol, 12(2), 175–190. doi:10.1517/17425255.2016.1125882 [PubMed: 26750630]

Madoff RD, & Fleshman JW (2004). American Gastroenterological Association technical review on the diagnosis and treatment of hemorrhoids. Gastroenterology, 126(5), 1463–1473. doi:10.1053/j.gastro.2004.03.008 [PubMed: 15131807]

Malysz J, Gibbons SJ, Saravanaperumal SA, Du P, Eisenman ST, Cao C, . . . Farrugia G. (2017). Conditional genetic deletion of Ano1 in interstitial cells of Cajal impairs Ca(2+) transients and slow waves in adult mouse small intestine. Am J Physiol Gastrointest Liver Physiol, 312(3), G228–g245. doi:10.1152/ajpgi.00363.2016 [PubMed: 27979828]

Mandala M, Heppner TJ, Bonev AD, & Nelson MT (2007). Effect of endogenous and exogenous nitric oxide on calcium sparks as targets for vasodilation in rat cerebral artery. Nitric oxide : biology and chemistry / official journal of the Nitric Oxide Society, 16(1), 104–109. doi:10.1016/j.niox.2006.06.007

McCallion K, & Gardiner KR (2001). Progress in the understanding and treatment of chronic anal fissure. Postgrad Med J, 77(914), 753–758. doi:10.1136/pmj.77.914.753 [PubMed: 11723312]

Murphy RA, & Rembold CM (2005). The latch-bridge hypothesis of smooth muscle contraction. Can J Physiol Pharmacol, 83(10), 857–864. doi:10.1139/y05-090 [PubMed: 16333357]

Nelson MT, Cheng H, Rubart M, Santana LF, Bonev AD, Knot HJ, & Lederer WJ (1995). Relaxation of Arterial Smooth Muscle by Calcium Sparks. Science, 270(5236), 633–637. doi:10.1126/science.270.5236.633 [PubMed: 7570021]

Ohkura M, Sasaki T, Kobayashi C, Ikegaya Y, & Nakai J. (2012). An improved genetically encoded red fluorescent Ca2+ indicator for detecting optically evoked action potentials. PLoS One, 7(7), e39933. doi:10.1371/journal.pone.0039933 [PubMed: 22808076]

Paez-Cortez J, Krishnan R, Arno A, Aven L, Ram-Mohan S, Patel KR, . . . Fine A. (2013). A new approach for the study of lung smooth muscle phenotypes and its application in a murine model of allergic airway inflammation. PLoS One, 8(9), e74469. doi:10.1371/journal.pone.0074469 [PubMed: 24040256]

Perez-Cornejo P, Gokhale A, Duran C, Cui Y, Xiao Q, Hartzell HC, & Faundez V. (2012). Anoctamin 1 (Tmem16A) Ca2+-activated chloride channel stoichiometrically interacts with an ezrin-radixin-moesin network. Proc Natl Acad Sci U S A, 109(26), 10376–10381. doi:10.1073/pnas.1200174109 [PubMed: 22685202]

Quignard JF, Frapier JM, Harricane MC, Albat B, Nargeot J, & Richard S. (1997). Voltage-gated calcium channel currents in human coronary myocytes. Regulation by cyclic GMP and nitric oxide. J Clin Invest, 99(2), 185–193. doi:10.1172/JCI119146 [PubMed: 9005986]

Rao SS (2004). Pathophysiology of adult fecal incontinence. Gastroenterology, 126(1 Suppl 1), S14–22. doi:10.1053/j.gastro.2003.10.013 [PubMed: 14978634]

Rattan s. (2005). The internal anal sphincter: regulation of smooth muscle tone and relaxation. Neurogastroenterology and Motility, 17(s1), 50–59. [PubMed: 15836455]

Rattan S. (2017). Ca2+/calmodulin/MLCK pathway initiates, and RhoA/ROCK maintains, the internal anal sphincter smooth muscle tone. Am J Physiol Gastrointest Liver Physiol, 312(1), G63–g66. doi:10.1152/ajpgi.00370.2016 [PubMed: 27932502]

Rattan S, Regan RF, Patel CA, & De Godoy MA (2005). Nitric oxide not carbon monoxide mediates nonadrenergic noncholinergic relaxation in the murine internal anal sphincter. Gastroenterology, 129(6), 1954–1966. doi:10.1053/j.gastro.2005.08.050 [PubMed: 16344064]

Rattan S, & Singh J. (2011a). Basal internal anal sphincter tone, inhibitory neurotransmission, and other factors contributing to the maintenance of high pressures in the anal canal. Neurogastroenterol Motil, 23(1), 3–7. doi:10.1111/j.1365-2982.2010.01629.x [PubMed: 21188800]

Rattan S, & Singh J. (2011b). Basal internal anal sphincter tone, inhibitory neurotransmission, and other factors contributing to the maintenance of high pressures in the anal canal. Neurogastroenterology and motility : the official journal of the European Gastrointestinal Motility Society, 23(1), 3–7. [PubMed: 21188800]

Sanders KM, Kito Y, Hwang SJ, & Ward SM (2016). Regulation of Gastrointestinal Smooth Muscle Function by Interstitial Cells. Physiology, 31(5), 316–326. doi:10.1152/physiol.00006.2016 [PubMed: 27488743]

Sharma N, Bhattarai JP, Hwang PH, & Han SK (2013). Nitric oxide suppresses L-type calcium currents in basilar artery smooth muscle cells in rabbits. Neurological research, 35(4), 424–428. doi:10.1179/1743132812Y.0000000129 [PubMed: 23540411]

Somlyo AP, & Somlyo AV (1994). Signal transduction and regulation in smooth muscle. Nature, 372(6503), 231–236. doi:10.1038/372231a0 [PubMed: 7969467]

Stamler JS, Sun QA, & Hess DT (2008). A SNO storm in skeletal muscle. Cell, 133(1), 33–35. doi:10.1016/j.cell.2008.03.013 [PubMed: 18394987]

Stewart AM, Cook MS, Dyer KY, & Alperin M. (2018). Structure-function relationship of the human external anal sphincter. Int Urogynecol J, 29(5), 673–678. doi:10.1007/s00192-017-3404-6 [PubMed: 28689239]

Sun J, Yamaguchi N, Xu L, Eu JP, Stamler JS, & Meissner G. (2008). Regulation of the cardiac muscle ryanodine receptor by O(2) tension and S-nitrosoglutathione. Biochemistry, 47(52), 13985–13990. doi:10.1021/bi8012627 [PubMed: 19053230]

Tan X, & Sanderson MJ (2014). Bitter tasting compounds dilate airways by inhibiting airway smooth muscle calcium oscillations and calcium sensitivity. Br J Pharmacol, 171(3), 646–662. doi:10.1111/bph.12460 [PubMed: 24117140]

Tsukada Y, Ito M, Watanabe K, Yamaguchi K, Kojima M, Hayashi R, . . . Saito N. (2016). Topographic Anatomy of the Anal Sphincter Complex and Levator Ani Muscle as It Relates to Intersphincteric Resection for Very Low Rectal Disease. Dis Colon Rectum, 59(5), 426–433. doi:10.1097/dcr.0000000000000565 [PubMed: 27050605]

van Helden DF, & Imtiaz MS (2003). Ca2+ phase waves: a basis for cellular pacemaking and long-range synchronicity in the guinea-pig gastric pylorus. J Physiol, 548(Pt 1), 271–296. doi:10.1113/jphysiol.2002.033720 [PubMed: 12576498]

Waniishi Y, Inoue R, Morita H, Teramoto N, Abe K, & Ito Y. (1998). Cyclic GMP-dependent but G-kinase-independent inhibition of Ca2+-dependent Cl- currents by NO donors in cat tracheal smooth muscle. J Physiol, 511 (Pt 3), 719–731. doi:10.1111/j.1469-7793.1998.719bg.x [PubMed: 9714855]

Yu K, Jiang T, Cui Y, Tajkhorshid E, & Hartzell HC (2019). A network of phosphatidylinositol 4,5-bisphosphate binding sites regulates gating of the Ca(2+)-activated Cl(−) channel ANO1 (TMEM16A). Proc Natl Acad Sci U S A, 116(40), 19952–19962. doi:10.1073/pnas.1904012116 [PubMed: 31515451]

Zbar Jayne, Mathur Ambrose, & Guillou. (2000). The importance of the internal anal sphincter (IAS) in maintaining continence: anatomical, physiological and pharmacological considerations. Colorectal Dis, 2(4), 193–202. doi:10.1046/j.1463-1318.2000.00159.x [PubMed: 23578077]

Zbar AP, Aslam M, Gold DM, Gatzen C, Gosling A, & Kmiot WA (1998). Parameters of the rectoanal inhibitory reflex in patients with idiopathic fecal incontinence and chronic constipation. Dis Colon Rectum, 41(2), 200–208. [PubMed: 9556245]

Zhang CH, Wang P, Liu DH, Chen CP, Zhao W, Chen X, . . . Zhu MS (2016). The molecular basis of the genesis of basal tone in internal anal sphincter. Nat Commun, 7, 11358. doi:10.1038/ncomms11358 [PubMed: 27101932]

Zhivotovsky B, & Orrenius S. (2011). Calcium and cell death mechanisms: a perspective from the cell death community. Cell Calcium, 50(3), 211–221. doi:10.1016/j.ceca.2011.03.003 [PubMed: 21459443]

ZhuGe R, Sims SM, Tuft RA, Fogarty KE, & Walsh JV Jr. (1998). Ca2+ sparks activate K+ and Cl- channels, resulting in spontaneous transient currents in guinea-pig tracheal myocytes. J Physiol, 513 (Pt 3), 711–718. [PubMed: 9824712]

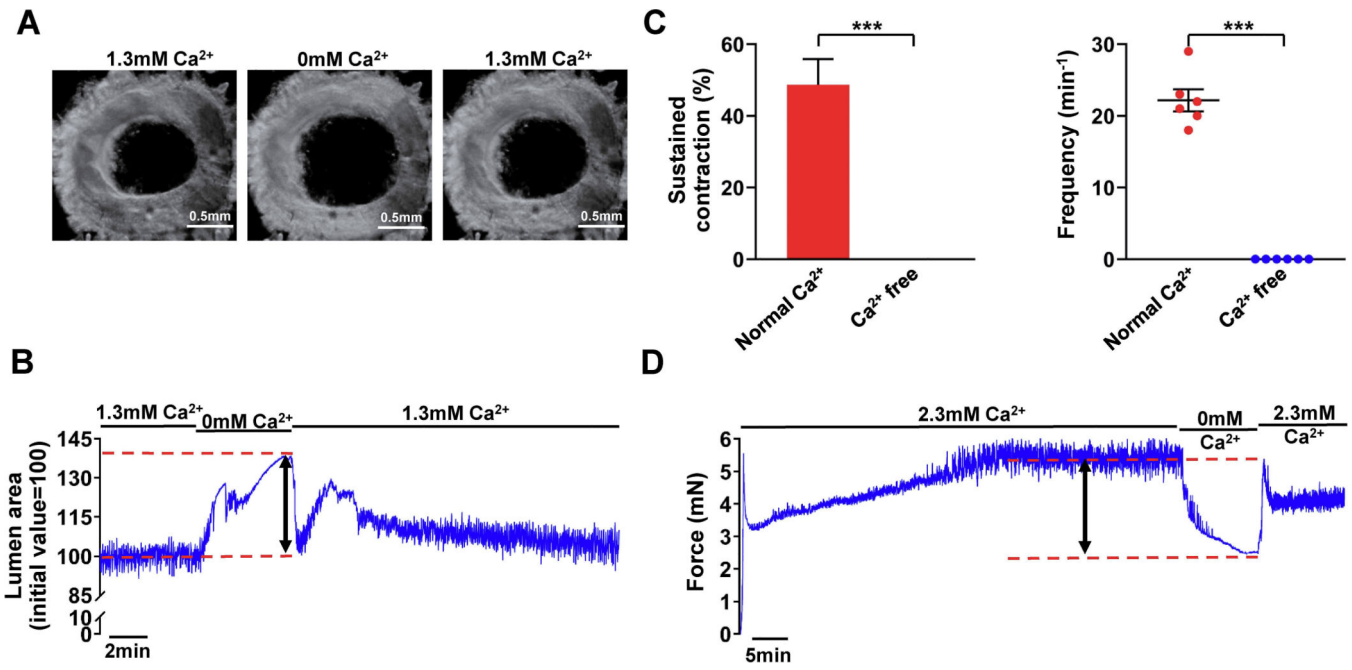

FIGURE 1:

The basal tone of internal anal sphincter (IAS) consists of phasic and sustained contractions. (a) Images of a mouse IAS slice under standard calcium medium (left), calcium-free medium (middle), and recovery from calcium-free medium (right). (b) Changes in the lumen area of an IAS slice in response to changes in extracellular calcium levels. (c) Quantification of sustained contraction (left panel) and phasic contraction (right panel) generated by IAS slices under isotonic condition ($n = 6$). (d) A representative example of sustained and phasic contractions produced by a mouse IAS strip under the isometric condition in response to the changes in extracellular Ca^{2+}. Note that (1) the difference between the two red dashed lines is defined as the sustained contraction of IAS slices (c), and of IAS strips (d), (2) phasic contractions are the much smaller, high frequency (~20/min) oscillations, and (3) the basal tone at rest in the presence of extracellular Ca^{2+} is the sum of sustained contractions and phasic contractions under both isotonic contraction (IAS slices) and isometric contraction (IAS strips). ***$p < .001$ by paired two-tailed Student's t test.

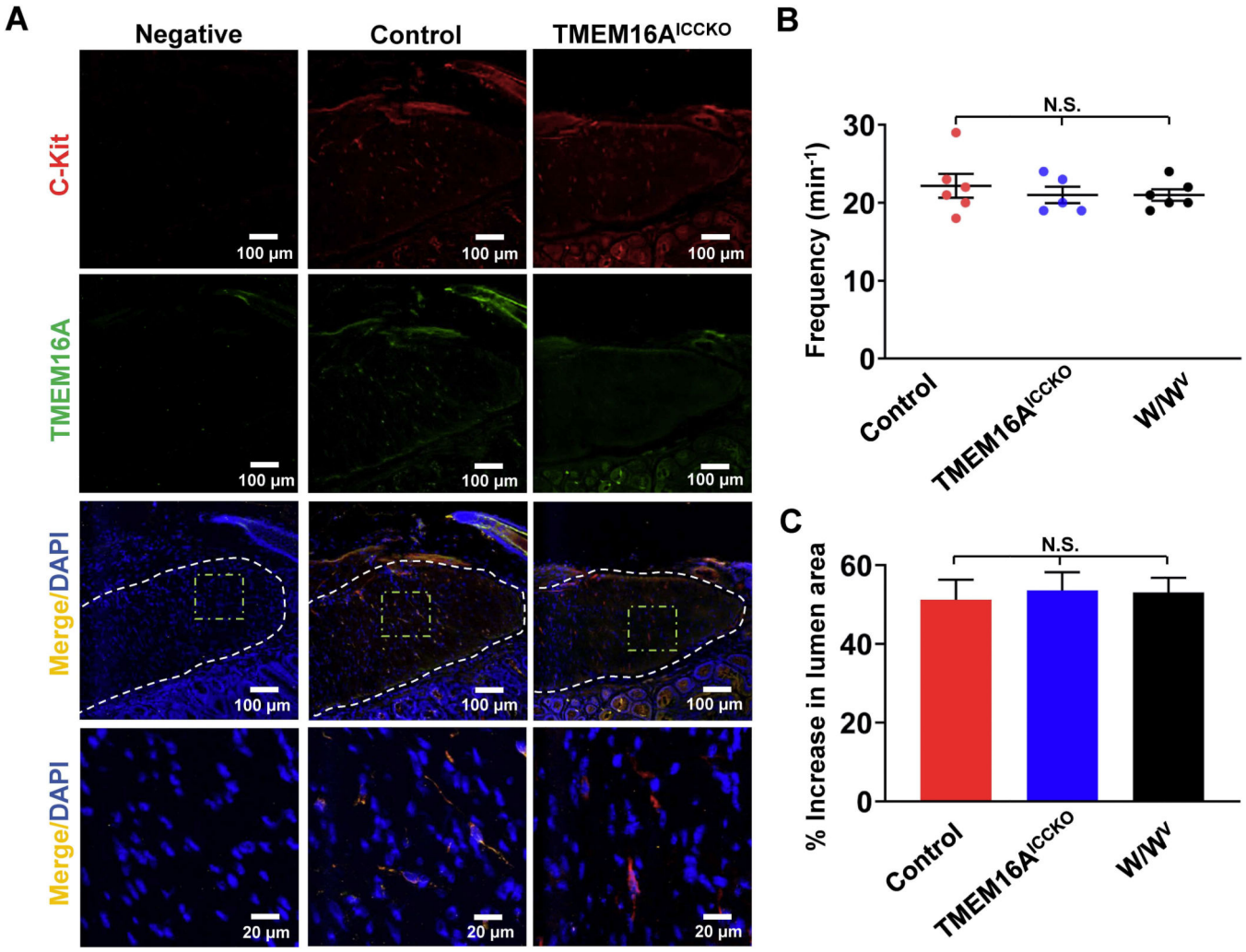

FIGURE 2:

TMEM16A deletion in c-kit positive interstitial cells of Cajal (ICC) does not affect IAS slices' contraction responses. (a) Immunohistochemistry of TMEM16A in mouse IAS. Red: c-Kit (a specific ICC marker); green: TMEM16A; blue: nucleus as revealed by DAPI. The fourth row shows enlarged views of the region within the square box on the third row. (b) Phasic contraction frequencies of IAS slices from control ($n = 6$), TMEM16A^{ICCKO} mice ($n = 5$), and W/W^{v} mice ($n = 6$). (c): Lumen area, sustained contraction of IAS slices from control ($n = 6$), TMEM16A^{ICCKO} ($n = 5$) mice and W/W^{v} mice ($n = 6$). N.S., not statistically significant by unpaired two-tailed Student's *t* test. DAPI, 4′,6-diamidino-2-phenylindole; IAS, internal anal sphincter.

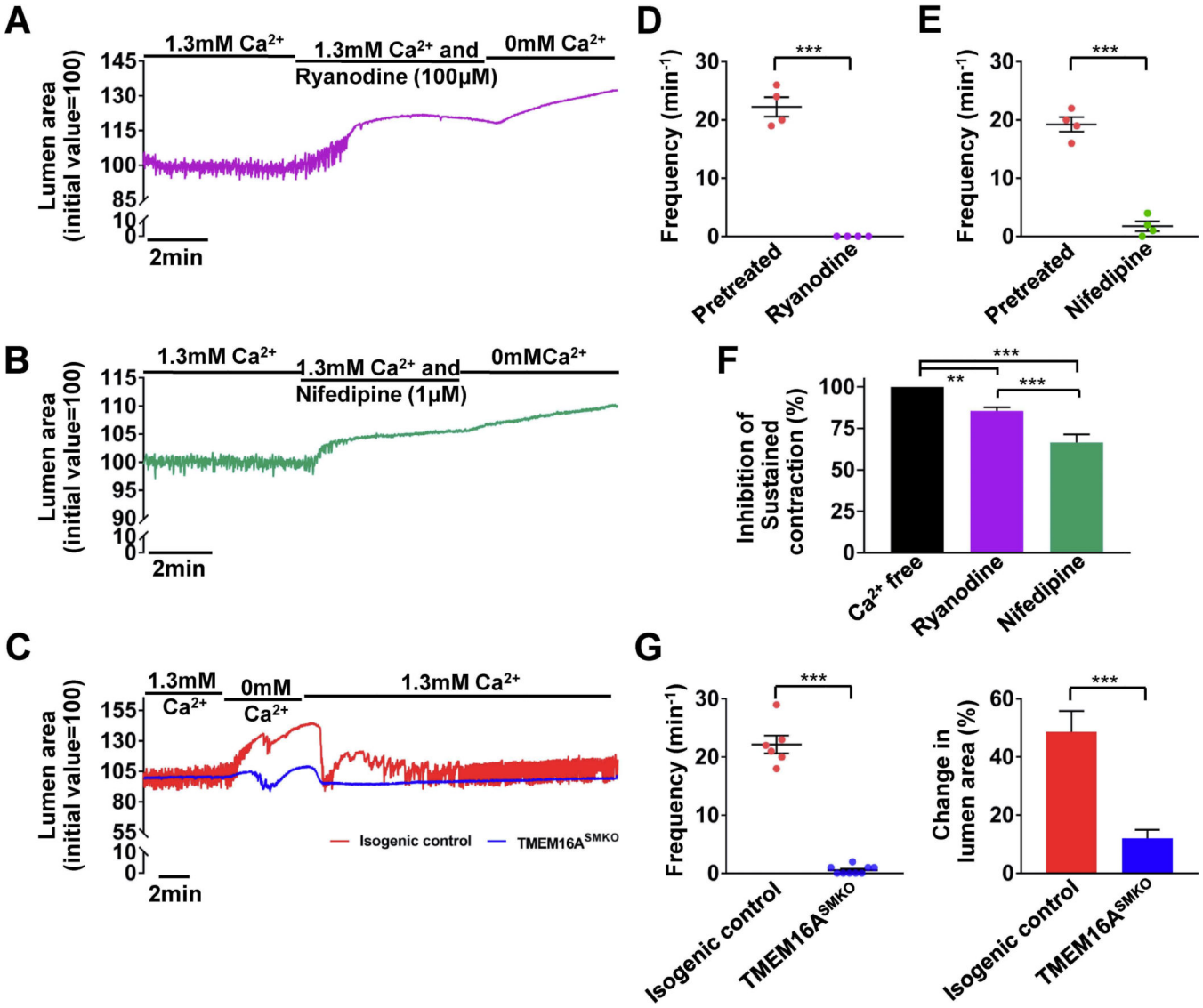

FIGURE 3:

The pharmacological and genetic characteristics of IAS contractile responses. (a) Dynamic effect of ryanodine on the phasic and sustained contraction of an IAS slice. (b) Dynamic effect of nifedipine on the phasic and sustained contraction of an IAS slice. (c) Representative time courses of contractile responses to changes in the extracellular Ca^{2+} in IAS slices from isogenic control mice and $TMEM16A^{SMKO}$ mice. (d,e) Summarized results of ryanodine and nifedipine effects on the phasic contraction frequency of IAS slices ($n = 4$ for each). (f) Summarized results on the effects of ryanodine ($n = 4$) and nifedipine ($n = 5$) on the sustained contraction of IAS slices (for Ca^{2+} free, $n = 5$). (g): Comparison of phasic (left) and sustained contraction (right) in IAS slices from isogenic control mice ($n = 6$) and $TMEM16A^{SMKO}$ mice ($n = 9$). $^{**}p < .01$; $^{***}p < .001$ by unpaired or paired two-tailed Student's t test. IAS, internal anal sphincterV

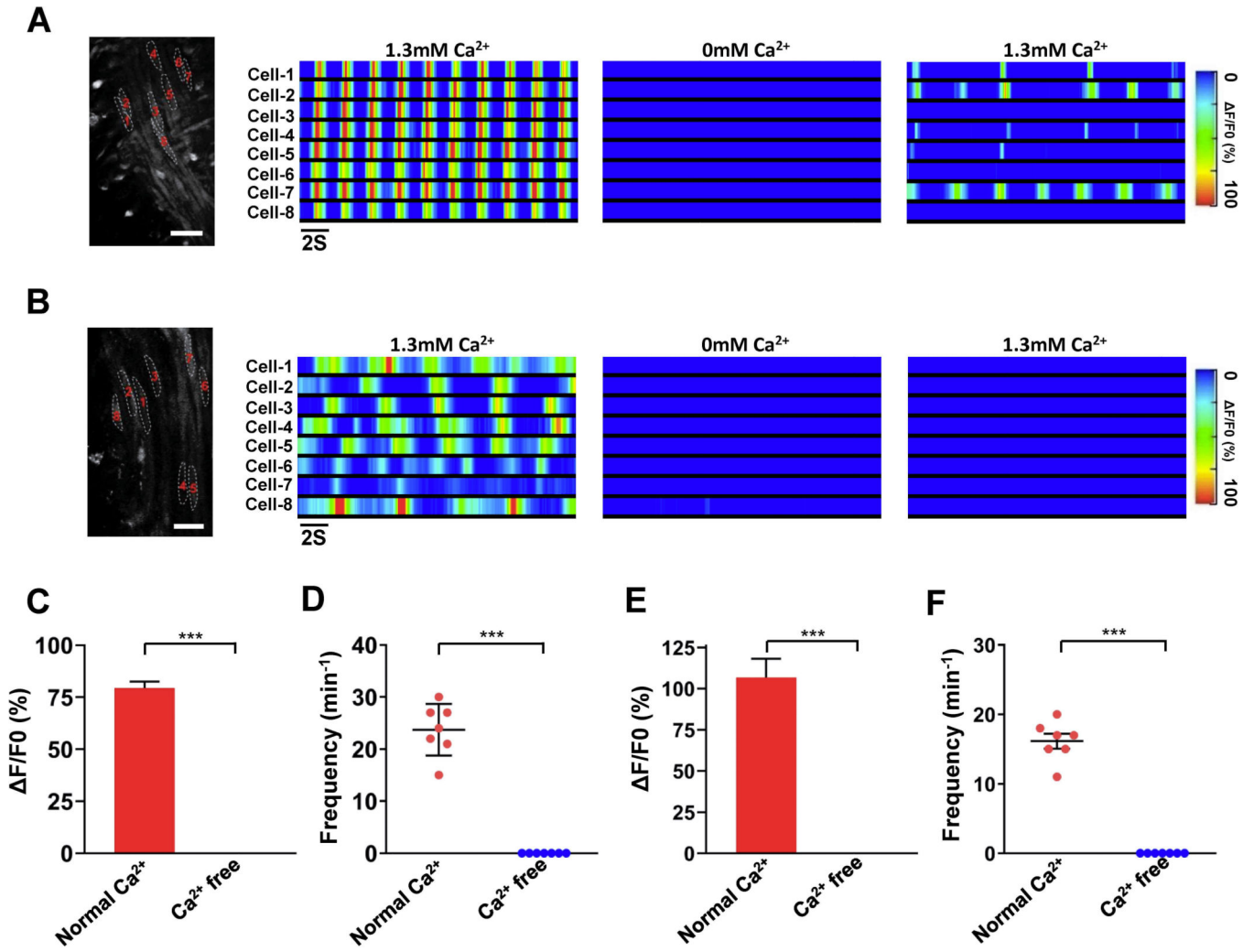

FIGURE 4:

IAS–smooth muscle cells (SMCs) exhibit synchronized Ca^{2+} oscillations (SCaOs) and asynchronized Ca^{2+} oscillations (ACaOs). (a) Kymographs of SCaOs in the presence of extracellular Ca^{2+} (left), in the last 20 s of 5 min Ca^{2+} free medium perfusion (middle), and in the last 20 s of 5 min Ca^{2+} restoration with Ca^{2+} containing medium (right). Cell id is labeled on the cells in the image on the far left panel, scale bar = 100 μm. (b) Kymographs of ACaOs in the cells in the presence of extracellular Ca^{2+} (left), in the last 20 s of 5 min Ca^{2+} free medium perfusion (middle), and in the last 20 s of 5 min Ca^{2+} restoration with Ca^{2+} containing medium (right). Cell id is labeled on the cells in the image on the far left panel, scale bar = 100 μm. (c, d) The effect of removing extracellular calcium on the (c) amplitude ($n = 12$) and (d) frequency ($n = 7$) of SCaOs. (e,f) The effect of zero extracellular calcium on the (e) amplitude ($n = 12$) and (f) frequency ($n = 7$) of ACaOs. All kymographs were taken during the same time interval. The graphs are the averaged whole-cell ΔF/F0 values, and this convention is applied to all the kymographs below. ***$p < .001$ by paired two-tailed Student's t test. IAS, internal anal sphincterV

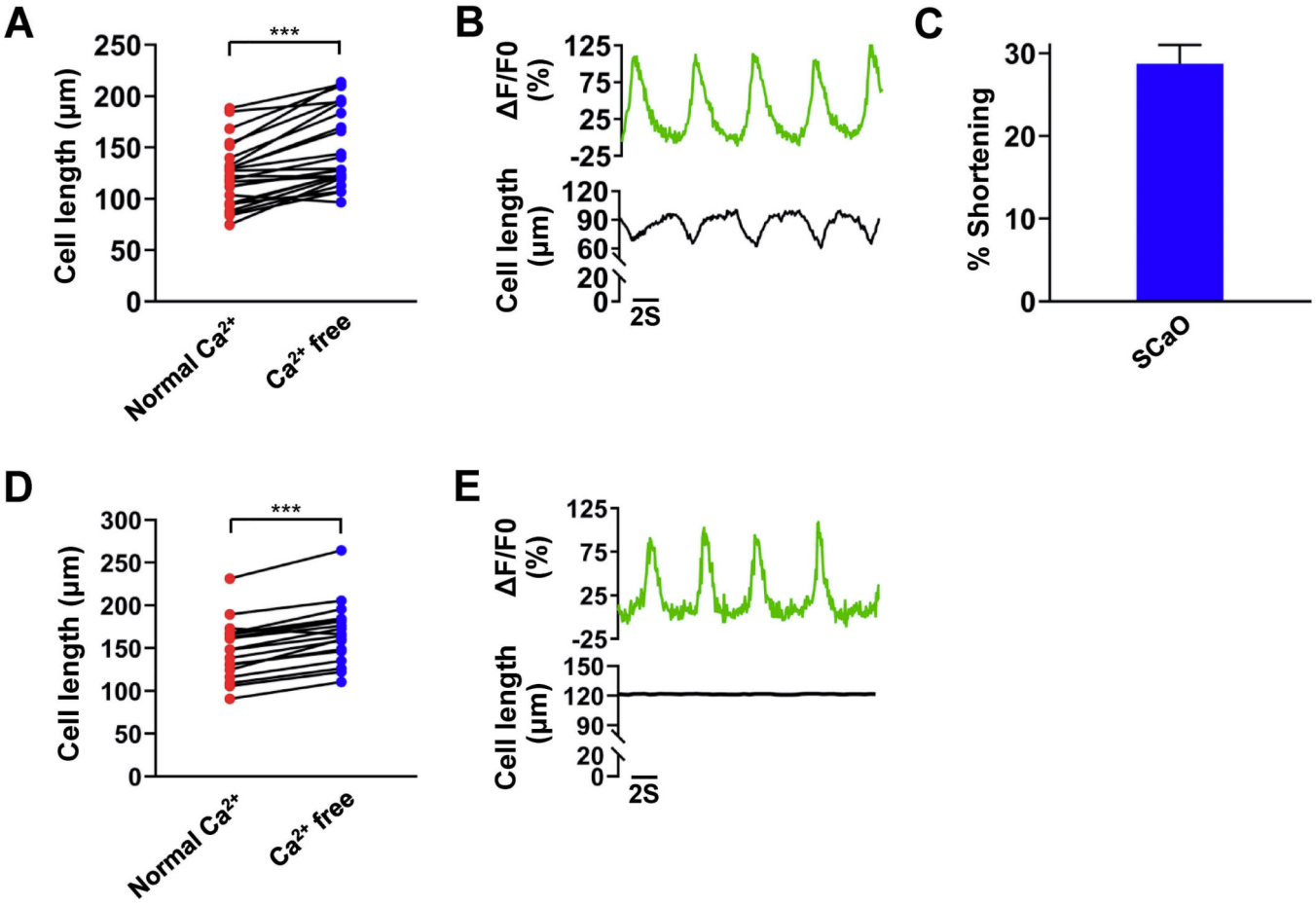

FIGURE 5:

SCaOs and ACaOs exert different roles in IAS–SMC Sustained Contraction and Shortening. (a) Changes in cell length of SCaOs in the steady-state in the presence of extracellular Ca^{2+} and its absence in IAS slices ($n = 24$). (b) SCaOs (upper trace) are associated with transient changes in the length (lower trace) in IAS–SMCs. (c) Summarized data on the maximal change in cell length caused by SCaOs ($n = 12$). (d) Change in cell length of ACaOs in the steady-state in the presence of extracellular Ca^{2+} and its absence in IAS slices ($n = 19$). (e) ACaOs (upper trace) do not change IAS–SMC length (lower trace). ***$p < .001$ by paired two-tailed Student's t test. ACaO, asynchronized Ca^{2+} oscillation; IAS, internal anal sphincter; SCaO, synchronized Ca^{2+} oscillation; ACaO, asynchronized Ca^{2+} oscillation; SMC, smooth muscle cell

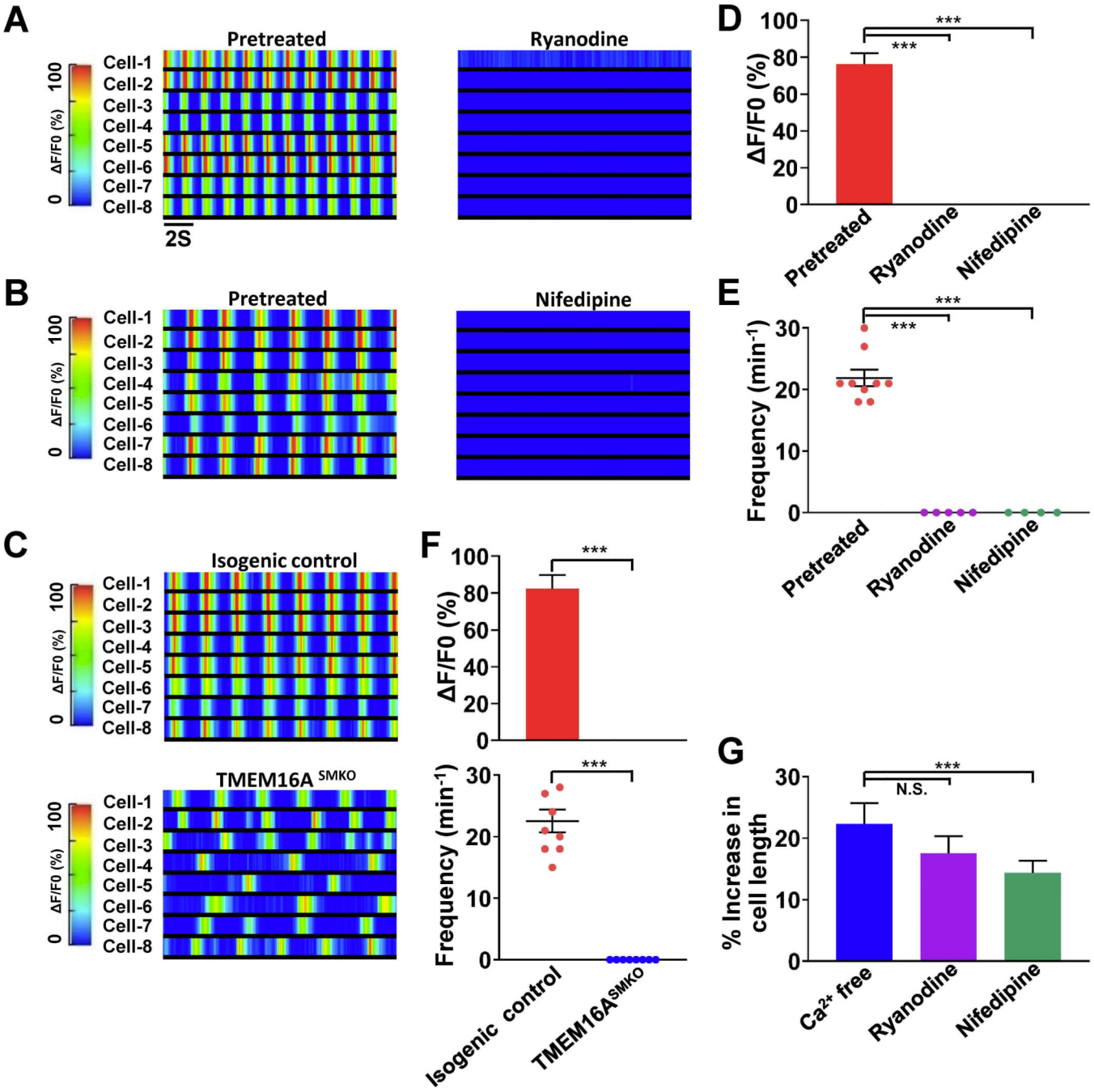

FIGURE 6:

The molecular mechanism underlies the generation of SCaO. (a,b) Kymographs showing the effect of ryanodine (a) and nifedipine (b) on SCaOs. (c) IAS slices from isogenic controls generated SCaOs (upper), while TMEM16A^{SMKO} mice produced no SCaOs but ACaOs (lower). (d,e) Summarized data on ryanodine (n = 5) and nifedipine (n = 4) effects on SCaO (d) amplitude and (e) frequency. (f) Summarized data on the amplitude (upper) and frequency (lower) of SCaOs in IAS slices from isogenic control mice (n = 8) and TMEM16A^{SMKO} mice (n = 8). (g) Summarized data on ryanodine (n = 13) and nifedipine (n

= 17) effects on the length of IAS–SMCs that generated SCaOs (for Ca^{2+} free, $n = 24$). The identifications of cells in (a), (b), and (c) are shown in Figure S8. ***$p < .001$ by paired or unpaired two-tailed Student's t test. ACaO, asynchronized Ca^{2+} oscillation; IAS, internal anal sphincter; NS, no statistical significance; SCaO, exhibit synchronized Ca^{2+} oscillation; SMC, smooth muscle cell

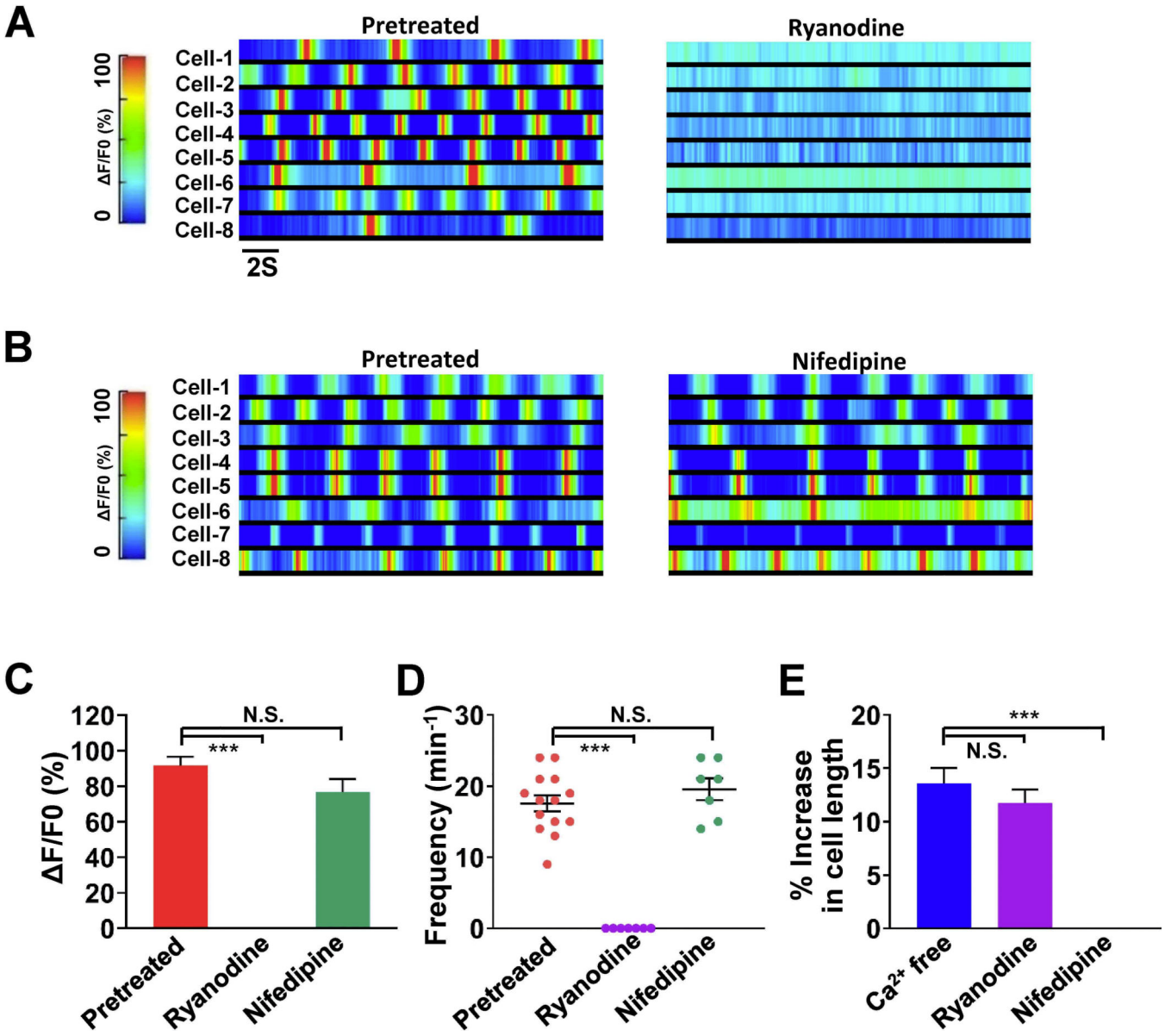

FIGURE 7:

The molecular mechanism underlies the generation of ACaOs. (a) Kymographs showing the effect of ryanodine on ACaOs. (b) Kymographs showing the effect of nifedipine on ACaOs. (c,d) Summarized data on ryanodine and nifedipine effects on ACaO (c) amplitude ($n = 7$ for each group) and (d) frequency ($n = 7$ for each group). (e) Summarized data on ryanodine ($n = 15$) and nifedipine ($n = 18$) effects on the length of IAS–SMCs that generated ACaOs (for Ca^{2+} free, $n = 19$). The identifications of cells in (a) and (b) are shown in Figure S8. ***$p < .001$ by unpaired two-tailed Student's t test. ACaO, asynchronized Ca^{2+} oscillation; IAS, internal anal sphincter;; NS, no statistical significance; SMC, smooth muscle cell

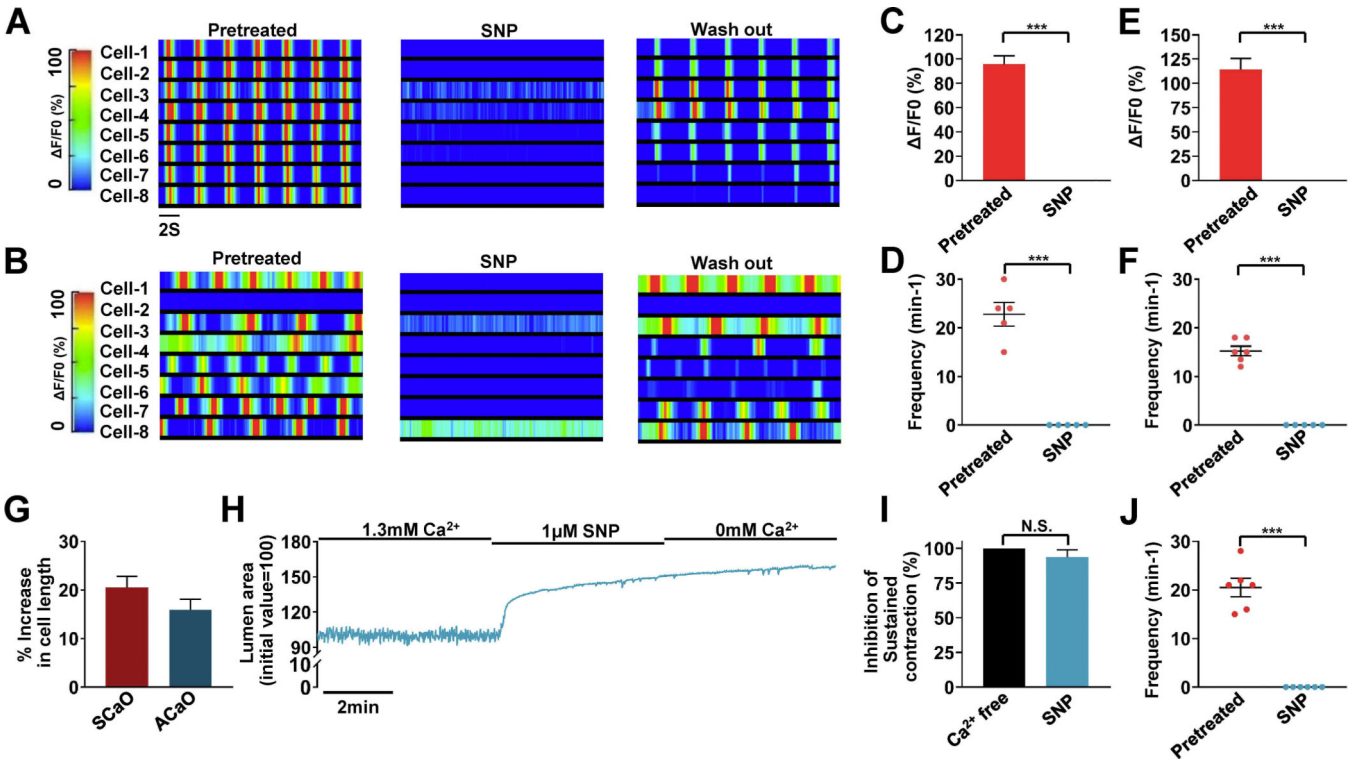

FIGURE 8:

Nitric oxide donor sodium nitroprusside (SNP) blocks both SCaOs and ACaOs to relax IAS. (a) A representative recording of the effect of SNP on SCaOs. (e) A representative recording of the effect of SNP on ACaOs. (c,d) Summarized data on SNP's effects on the (c) amplitude ($n = 5$) and (d) frequency ($n = 5$) of SCaOs. (e,f) Summarized data on the effect of NO on the (e) amplitude ($n = 5$) and (f) frequency ($n = 5$) of ACaOs. (g) Summarized data on SNP-induced relaxation of IAS–SMCs that produced SCaOs ($n = 15$) or ACaOs ($n = 15$). (h) The lumen change of an IAS slice in response to SNP and the removal of extracellular calcium. (i,j) Summarized data for the experiments showed on (h; $n = 5$ for both SNP and Ca^{2+} free). The identifications of cells in (a) and (b) are shown in Figure S8. ***$p < .001$ by paired or unpaired two-tailed Student's t test. ACaO, asynchronized Ca^{2+} oscillation; IAS, internal anal sphincter; NS, no statistical significance; SCaO, synchronized Ca^{2+} oscillation; SMC, smooth muscle cell

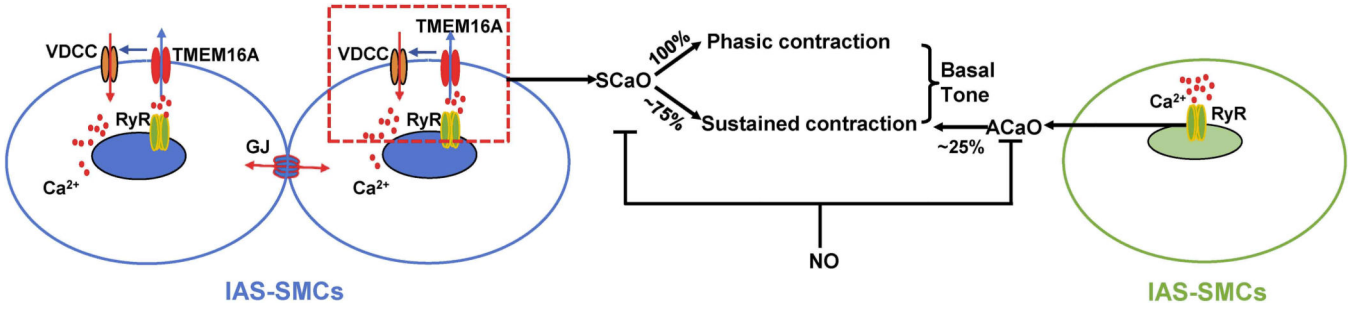

FIGURE 9:

A model on IAS basal tone generation and maintenance. See the text for the details. ACaO, asynchronized Ca^{2+} oscillation; IAS-SMCs, internal anal sphincter smooth muscle cells; GJ, gap junction; NO, nitric oxide; RyR, ryanodine receptor; SCaO, synchronized Ca^{2+} oscillation; VDCC, voltage-dependent calcium channel